Application of Lagrangian Formulation to Predict the Positioning Error of Parallel Manipulator Under External Loads

MUHAMMAD SOHAIL
NUST201362430MCEME35113F

Supervisor
DR. SAJID ULLAH BUTT

DEPARTMENT OF MECHANICAL ENGINEERING
COLLEGE OF ELECTRICAL & MECHANICAL ENGINEERING
NATIONAL UNIVERSITY OF SCIENCES AND TECHNOLOGY
ISLAMABAD
JUNE, 2016

Application of Lagrangian Formulation to Predict the Positioning Error of Parallel Manipulator Under External Loads

MUHAMMAD SOHAIL
NUST201362430MCEME35113F

A thesis submitted in partial fulfillment of the requirements for the degree of
MS Mechanical Engineering

Thesis Supervisor:
DR. SAJID ULLAH BUTT

Thesis Supervisor's Signature: _____

DEPARTMENT OF MECHANICAL ENGINEERING
COLLEGE OF ELECTRICAL & MECHANICAL ENGINEERING
NATIONAL UNIVERSITY OF SCIENCES AND TECHNOLOGY,
ISLAMABAD
JUNE, 2016

Declaration

I certify that this research work titled *"Application of Lagrangian Formulation to Predict the Positioning Error of Parallel Manipulator Under External Loads"* is my own work. The work has not been presented elsewhere for assessment. The material that has been used from other sources it has been properly acknowledged / referred.

Signature of Student

MUHAMMAD SOHAIL

NUST201362430MCEME35113F

Language Correctness Certificate

This thesis has been read by an English expert and is free of typing, syntax, semantic, grammatical and spelling mistakes. Thesis is also according to the format given by the university.

Signature of Student

MUHAMMAD SOHAIL

NUST201362430MCEME35113F

Signature of Supervisor

Copyright Statement

Acknowledgements

Before beginning this manuscript, I would like to express my gratitude to Allah SWT for all blessing and benevolence which helped me to complete this task in terms of integrity and completeness. I would also like to thank people who have helped and guided me in this research and provided all possible assistance throughout the time of working on the thesis. It is a pleasure for me to thank those who made this thesis possible.

I gratefully thank my thesis supervisor, Assistant Professor Dr. Sajid Ullah Butt for his extended support and time throughout the thesis work. He was always available for help with his kind remarks. His continuous support, co-operation and encouragement were the keys for successful completion of this research work. I am also thankful for his tireless efforts during the review of the manuscript. In short, without his guidance, support and precious time, this work was impossible for me.

I would also like to express special thanks to Assistant Professor Dr. Hasan Aftab Saeed for his invaluable advice based on his expertise in FEA, during development of the analytical model proposed in this thesis, his knowledge helped pave way when I was struck and allowed me to work in a manner which was productive.

It is an honour for me to thank Assistant Professor Dr. Imran Akhtar, who always gave high-quality advices and discover important questions in my research which needed further investigations. From him I learned, how to write high-quality scientific works.

I am grateful to Associate Professor Dr. Aamer Ahmed Baqai for being an external member of my Guidance and Evaluation Committee (GEC) and for taking time from his tough schedule to attend my thesis presentations. I am really obliged for letting my defence be an enjoyable moment and for his brilliant comments and suggestions.

I would like to thank the entire honourable faculty and staff of Mechanical Department of College of E & ME whose professional approach and vision groomed me as a sound person both technically and morally.

The last and most important thanks goes to my family, who always supported me in all my pursuits. I would like to thank them for all their love and encouragement.

To my beloved parents, teachers and siblings…

Abstract

In last few decades, parallel manipulators have become an essential tool for many industries due to their high speed, accuracy, payload, stiffness and precision. These features make parallel manipulator ideal for jobs like, robotic surgery, precise manufacturing, missile launching and flight simulation, but precise part positioning on parallel manipulator is a challenging task in industry. With errors in position, one can never achieve the required quality of the part. In this work, our main focus is to find out positioning errors of a hexapod platform that are caused while machining. Legs will be considered elastic while the platform, part and leg-platform contacts will be considered rigid bodies. All legs are assumed to be 3D massless elastic trusses. When the load is applied on the part placed on the platform, its position may change due to elasticity of the manipulator. Lagrange formulation is used to calculate the positioning error of the platform as a result of machining forces and torques. A generalized algorithm is established, using Mathematica®, which gives us the positioning error of "n" legged system and for any initial orientation of the platform. In the second part, Natural frequencies of Stewart Platform are calculated from results generated in first part. The proposed methodology is applied on H-840 Hexapod designed and manufactured by Physik Instrumente. The Hexapod is designed and modelled in CATIA® and results are validated with Finite Element Analysis, as well as, from the literature.

Key Words: *Stewart Platform; Parallel Manipulator; Hexapod; Lagrangian Formulation; 3D-Trusses; Finite Element Analysis; 3D Stiffness Matrix*

Table of Contents

List of Figures

List of Tables

List of Abbreviations

DOF	:	Degrees of Freedom
FE	:	Finite Element
FEA	:	Finite Element Analysis
FEM	:	Finite Element Method
GSP	:	Gough Stewart Platform
HTM	:	Homogeneous Transformation Matrix
MSA	:	Matrix Structural Analysis
PI	:	Physik Instrumente
PM	:	Parallel Manipulator
PKM	:	Parallel Kinematic Machines
SP	:	Stewart Platform
VJM	:	Virtual Joint Method
YPR	:	Yaw, Pitch, Roll Transformation

List of Symbols

ΔX_P, ΔY_P, ΔZ_P:	Linear displacement in point "P" on the platform (unknown)
$\Delta\alpha$, $\Delta\beta$, $\Delta\gamma$:	Angular displacement of platform under load along Z, X and Y axis (unknown)
ΔX_i, ΔY_i, ΔZ_i:	Displacement vector of i^{th} leg transformed in terms of six unknown displacement vector
ΔX_f, ΔY_f, ΔZ_f:	Displacement of point of action of force transformed in term of six unknown variables
x_P, y_P, z_P:	Coordinates of "P" (Input)
x_i, y_i, z_i:	Coordinates of point contact of i^{th} leg on platform
x_{fp}, y_{fp}, z_{fp}:	Coordinates of point of application of force
Fx_i, Fy_i, Fz_i:	X, Y and Z components of i^{th} applied force
Mx, My, Mz:	Components of moment applied due to cutting tool
λx_i, λy_i, λz_i:	Components of unit vector of i^{th} leg
R_P:	Radius of platform
R_b:	Radius of base
r:	Cross sectional radius of leg
l_0:	Initial length of leg (Input)
n:	Total number of legs (Input)
θ_P:	Legs arrangement angle on the platform
θ_B:	Legs arrangement angle on the baseplate
E:	Modulus of elasticity of legs
$[K_i]$:	Stiffness matrix of i^{th} leg
k_{ij}	(i,j) component of global stiffness matrix
pe_i:	Potential energy of i^{th} leg
PE:	Overall Potential Energy of the Hexapod
KE:	Overall Kinetic Energy of the Hexapod
W:	Overall work done by applied forces
q_i:	Six DOF of platform $\{q_1, q_2, q_3, q_4, q_5, q_6\} = \{\Delta X, \Delta Y, \Delta Z, \Delta\beta, \Delta\gamma, \Delta\alpha\}$

CHAPTER 1: INTRODUCTION

Manipulators are backbone of modern industry. With respect to architecture, industrial manipulators are divided into two main groups; Serial manipulators and Parallel manipulators. In serial manipulators, links are connected in serial with each other, while in parallel manipulators all links have common base and platform. A third type not as famous as serial and parallel manipulators called Hybrid manipulator is available, it is combination of advantages of both the manipulators; like, wider space of serial manipulators and precision of parallel manipulators.

1.1 Serial Manipulator

Serial manipulators, shown in figure 1.1, possess serial kinematic chains composed of rigid links and is shaped by actuated joints. These joints can be either rotational and / or translational. The great benefit of serial robots is its large workspace with respect to its volume and space occupied at work. As serial manipulators have open kinematic structure, all errors are accumulated and amplified from end effector to base. Furthermore, it is difficult to get high stiffness and dynamic properties simultaneously. For instance, manipulators with high stiffness are usually heavy and cannot deliver high speed. Moreover, their own weight induces significant undesirable stresses in actuated joints that reduces allowable payload. On the other hand, serial manipulators with light weight links have lower stiffness so it cannot provide high payload because of significant compliance errors. These drawbacks decrease efficiency and application areas of serial manipulators. Based on kinematics, serial manipulators are further divided into three main groups; SCARA, Articulated and Cartesian manipulators as shown in figure 1.1.

(a) Articulated Robot (b) SCARA Robot (c) Cartesian Robot

Figure: 1.1 Serial Manipulator

1.2 Parallel Manipulator

The parallel manipulators (also called parallel kinematic machines (PKM)) possess closed loop structure with platform linked to base via several rigid links (Merlet 2000). The most common parallel manipulators are shown in figure 1.2. The kinematic chains are composed of several links that are connected by passive and / or actuated joints, either rotational and / or translational. Such kinematics offers advantages, like; highly rigid structure, high stiffness, high dynamic capacities and reliable accuracy (Tlusty, *et al.* 1999; Ph Wenger, *et al.* 1999; Philippe *et al.* 2007). Another important advantage of parallel robots is better accuracy, because here the position and orientation errors of each kinematic chains is averaged by the end platform, which in case of serial manipulator were accumulated.

Figure: 1.2 Parallel Manipulators

In this thesis, an analytical model is proposed. The model calculates relative positioning error of the static platform of the Hexapod under external loadings with reference to unloaded configuration of the platform, it is assumed that whole positioning error is due to elasticity of legs which are taken to be 3D elastic trusses. The proposed algorithm is formulated for "n" legged Hexapod and generic for any number of external forces and torques. The algorithm established in Mathematica®, calculates linear and angular displacements of the platform, along with, 3D stiffness matrix of the system.

1.3 Motivation and Methodology

Higher stiffness with accuracy and speed make the parallel manipulators favourite for many jobs like, robotic surgery, precise manufacturing, missile launching and flight simulation. All the features ruin out if there is error in the position of part placed on the platform of manipulator, so the positioning error requires special attention while using these manipulators.

The positioning errors could evolve due to elasticity of legs, joints and actuators. In this work, our main focus is to find out positioning errors of a hexapod platform that are caused while machining. The working methodology of proposed analytical model will be introduced in this section. The model gets inputs form Excel® spreadsheet, which includes machining forces and their positions in the platform, Material properties of Hexapod, Radiuses of legs, Platform and the Base and Legs' arrangement angles. Using the inputs, algorithm calculates Kinetic Energy, total Potential Energy and Work done by external forces for itself and gives; the six unknown displacements of the platform, the Stiffness Matrix and Natural Frequencies along with corresponding mode shapes. A detailed methodology, based in following points, is described in Chapter 3.

- Positioning error due to deformation of elastic legs
- Elastic Potential Energy
- Inertial Kinetic Energy
- Total Work done by External forces
- Displacement of platform under load
- Study of Natural Frequencies and Mode shapes

1.4 Implementation of Proposed Model

The proposed techniques for displacement calculation of Hexapod (particularly Stewart Platform) is validated by Finite Element Analysis. A Stewart Platform (H-840) designed and manufactured by Physik Instrumente is modelled, simulated and analysed in CATIA®, displacements of platform from both the techniques are compared (Chapter 5), to verify the first part of thesis. The second part, that includes the 3D Stiffness Matrix is validates by solving a case study, already solved in published literature. It worth mentioning, the Stiffness Matrix is also validated in CATIA® by comparing the Natural Frequencies of the system, as calculated Stiffness Matrix is used for calculation of Natural Frequencies.

1.5 Outline of Thesis

The thesis is structured in 4 chapters and a conclusion. After the introduction, a detail of selected literature is explained in chapter 2. The chapter 2 begins with introduction to Serial and Parallel Manipulators. A comprehensive detail of errors in parallel manipulates with common approves to compensate these error from available literature is explained. In Stiffness

section, stiffness modelling approaches are discussed followed by the stiffness of Stewart Platform.

Chapter 3 presents the proposed analytical model for calculation of displacements and Natural Frequencies. It starts with the introduction of Lagrange equation, solution of which will give the required results. In other sections, each required part of Lagrange equation is calculated. The calculations involve, calculation of total elastic potential energy due to elasticity of each massless leg, the Inertial kinetic energy due to mass of rigid platform and total work done due to external loads. The method for calculation of Natural Frequencies and mode shapes are also presented in the end before conclusion of cahpter3.

In Chapter 4, a case study is solved by proposed methodology, as well as, by modelling and analysing a Stewart Platform with same dimensions in CATIA®. The working of the algorithm formulated in Mathematica®, form file exporting to importing and inputs to outputs, each step is explained in detail. In remaining sections of chapter 4, steps involved in designing and modelling of Stewart Platform in CATIA® are described. Before chapter's conclusion, results from both techniques are compared and a numerical study form published literature is solved to testify the proposed work.

In 5^{TH} chapter, the obtained results are plotted to check out the effect of single variable on the displacement error of the Stewart Platform, based on these plots a limit is defined on design variables to reduce positioning error in platform of the Hexapod.

In the final conclusion, the advantages and demerits of the proposed technique are discussed which is followed by the future works and references of the work cited in the thesis.

CHAPTER 2: LITERATURE REVIEW

In this chapter, limitations, advantages and specifications of robotic errors during machining applications with analysis on compensation techniques are reviewed. The key stress of this chapter is to review existing literature on stiffness modelling approaches for parallel manipulators. Finally, the goal and problem for this work is defined.

2.1 Why Parallel Manipulator?

As the parallel manipulators are composed of several links connecting single platform, so highly rigid structure with stiffness, and accuracy is expected (Tlusty, *et al.* 1999; Ph Wenger, *et al.* 1999; Philippe *et al.* 2007). Using special arrangement of kinematic chains, it is possible to ensure high stiffness and high dynamic properties, simultaneously. These capabilities make the parallel robots highly suitable for high-speed machining. However, parallel robots have very complex limited working envelop (Shoval *et al.* 2001). Some researchers tried to overcome this issue by combining different types of joints, the achieved success resulted in decrease of load carrying capability of parallel manipulator (Dombiak, *et al.* 2000; Horin, *et al.,*1999). Performance of parallel manipulator (maximum speeds, accuracy and rigidity) essentially differs from point to point and also depend on the moving directions. Other disadvantages of parallel manipulators include their large footprint-to-workspace ratio (except the Tricept robot which requires less space) and small range of motion because of parallel configuration. These are the main obstacles for the machining applications of parallel robots (Kim *et al.* 1997; Rehsteiner *et al.* 1999).

At present, there are variety in parallel manipulators. Depending on the architecture, they may be divided into two groups that differ by the type of joints used between the base-platform and the serial chains (Chablat *et al.* 2003). The first group contains manipulators with fixed base points and variable length of legs. Mostly robots belonging to this group implement the Stewart-Gough architecture, have 6 degrees of freedom and are called Hexapods. They provide high precision and accuracy, good stiffness and high load/weight ratio. Due to these essential advantages, Hexapods are often used in flight simulators, precision machining, surgical robots, and other areas. By variation of the link lengths, Hexapods may satisfy both small and large workspace, but increasing of the link's length directly effects the accuracy of manipulator. The main technical issue of Hexapod is high friction of the ball joints. Typical examples of parallel manipulators belonging to the first group includes VARIAX, HEXA,

(a) HEXA – High speed robot

(b) VARIAX (Gidding & Lewis)

(c) Trocept (Neos-Robotics)

(d) Tripod - microrobot

Figure: 2.1 Parallel Manipulator (Group - I)

Tricept, Tripod and Delta manipulators are shown in figure 2.1 (Geldart *et al.* 2003; F. Pierrot, *et al.* 1991; Francois Pierrot *et al.* 2009; Zhang *et al.* 2005; Tsai *et al.* 2000).

The second group includes manipulators with foot points sliding on linear joints. Robots of second group (figure 2-2) differ by the number of actuated translational axis and their location with respect to each other, as well as, by the type of links connecting the base and moving platforms. Typically, this group has 5 or 6 degrees of freedom (Hexaglide, HexaM) but 3 degrees of freedom translational manipulators also exists in this family (Orthoglide) that employ parallelogram-based links similar to Delta robots (Toyama *et al.* 1998; Chablat *et al.* 2003). The robots of the second group are attractive for machining application due to their lower moving mass compared to the hexapods and tripods. However, to ensure large workspace, such robots require large volumes to operate and occupy essential floor space.

(a) HexaM

(b) Orthoglide

(c) Hexaglide

Figure: 2.2 Parallel Manipulator (Group – II)

Hence, parallel robots provide large number of benefits as compared to the serial ones, which promote them for quick and highly precise machining works. Due to this reason, they have already been employed in commercial machining centres.

2.2 Errors in Parallel Manipulator

Accuracy of manipulators depends on many factors, but those relating to manufacturing tolerances are crucial of all because with these errors the nominal machining accuracies can never be achieved, these errors are referred as geometrical errors, other important factor includes the deflection of end effector under machining forces and torques, these errors are called compliance errors.

2.2.1 Classification of Errors

Precision of the manipulator is usually described by three different performance measures: the resolution, repeatability and accuracy. The resolution determines the minimum increment that the manipulator can make. Repeatability is a feature of manipulator due to which it retracts its initial position and orientation. Finally, manipulator's accuracy (also referred as absolute accuracy) is the proficiency of manipulator to stop at exactly required location in Cartesian space. (Kevin *et al.* 2000).

Khalil *et al.* (2002) and Paziani *et al.* (2009) classified main causes of positioning errors of parallel manipulator in two main groups: geometrical and non-geometrical ones. Klimchik (2011) proposed a detailed classification of errors in manipulators, which is presented in figure 2.3. It is important to note, these errors can be both independent and correlated but for study purposes the errors are treated sequentially, considering them to be independent of each other. According to Elatta *et al.* (2004) in applications where the machining forces and torques are small in magnitude, the main source of errors in an accuracy of manipulator is due to geometrical errors, almost 90% of the total error in such cases is due to poor geometry of manipulator. The mismatching of nominal values with real values of parameters (like; links and joints etc.) are significant in these errors. This kind of error arises due to different origin values in actuator coordinates (actual system) and the mathematical model programmed in comptroller, this error is referred as joint offsets; it can also occur due to imperfections during assembling of different parts and due to transformation of local frames assumed with each component, generally these components are expected to be perfectly coordinated and allied. It worth mentioning, the geometrical errors are independent of the configuration of manipulator, however, it's effect on the positional accuracy depend on end effector. At present, there are large number of sophisticated techniques, capable of recognizing and abolishing different imperfections between geometrical parameters. However, this type of error can also be compensated using adjusted input provided to controller of the system, in some other cases, direct adjustments are also made in the geometrical parameters of the model being used in the robot controller system. (Veitschegger *et al.* 1986; Roth *et al.* 1987; Bennett *et al.* 1991; Mirman *et al.* 1992; Daney *et al.* 2006; Dolinsky *et al.* 2007; Hollerbach *et al.* 2008).

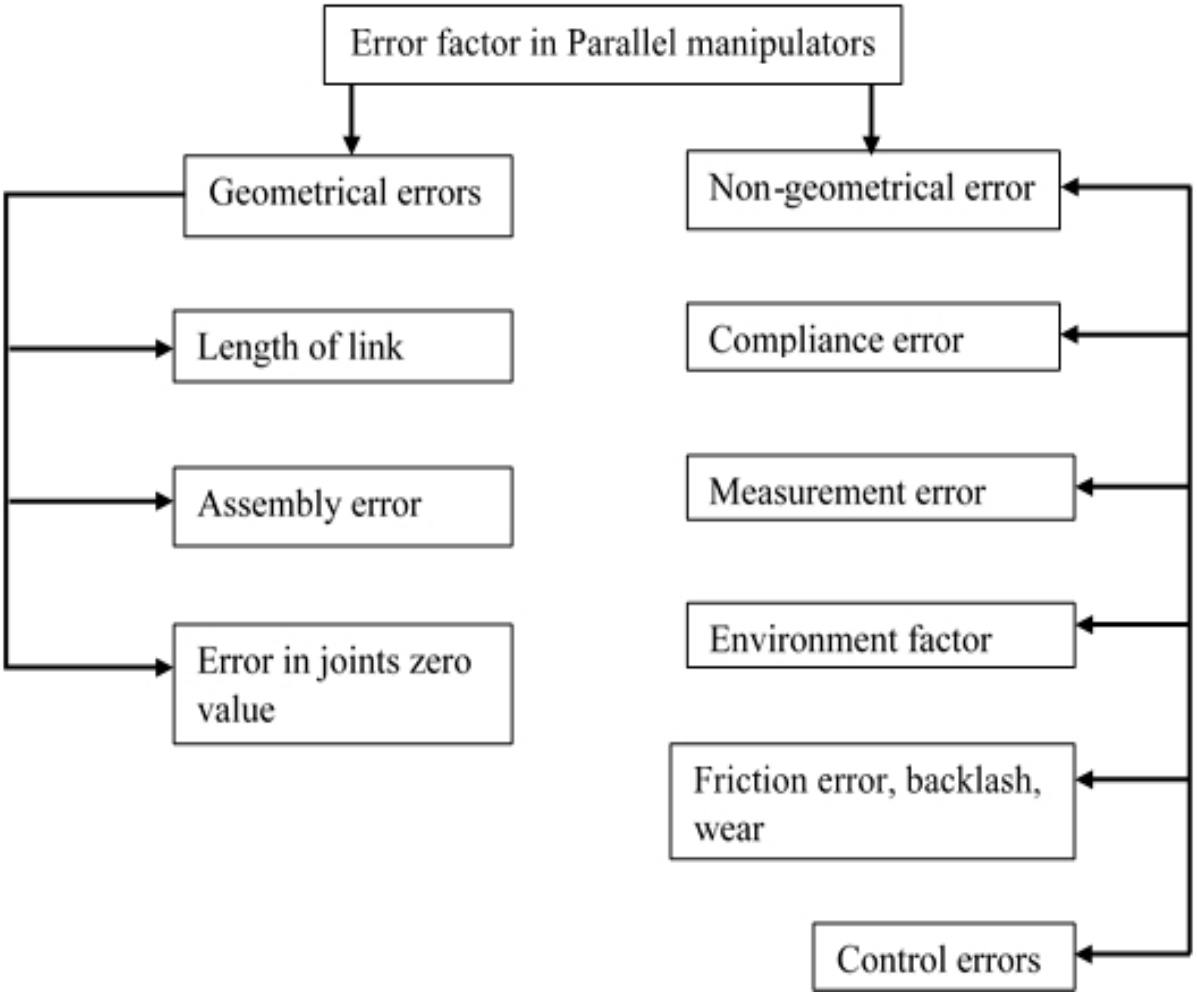

Figure: 2.3 Positioning Errors in Manipulators

In some scenarios, the geometrical errors are dominated by non-geometrical errors, due to different reasons (Gong *et al.* 2000; Cui *et al.* 2006; Bogdan *et al.* 2009). There are few errors due to interaction of tool on workpiece, these errors can cause deformation of components (like; legs, platform and joints etc.) of manipulators. These errors are called compliance errors, which will be main focus of this thesis**.** (Meggiolaro *et al.* 2005)**.** Likewise, the surrounding conditions like; temperature, atmospheric pressure etc., also affect the physical properties of the system's components, this leads to unwanted variations in deformable components. In the normal working environment, the inaccuracies due to compliance are the weightiest. The compliance errors are particularly significant for heavy systems with relatively low stiffness. The external forces and torques from the machining process produce significant deformations in system that cannot be ignored during precise manufacturing. In such cases, the geometrical errors are overlooked by the compliance error due to their greater impact on the positioning accuracy of system. Designers of parallel manipulators pay great attention on the

issue, while optimizing the dynamic capabilities and stiffness properties of manipulator (Cheboxarov *et al.* 2000).

The compliance error constitutes: *(a)* applied loadings and *(b)* Stiffness of system. In addition to external machining forces, sometimes, it is essential to consider the impact of the weight of links, the gravitational pull compensation mechanisms, as well as, pre-loadings in the passive joints that are introduced in order to eradicate backlash error from the system. The compliance error is configuration dependant so it differs all over the working space. However, relevant modelling and compensation techniques are still under study (Ramesh *et al.* 2000; Dow *et al.* 2004; Bera *et al.* 2011).

2.2.2 Compensation of the Errors

To get a reliable machine with minimum errors, the errors stated above must be compensated. The basic approach in the error's compensation is the absolute position feedback in which the location of end effector in global coordinates is obtained by addition of sensors in joints and links of manipulator. Main benefit of this technique includes, capability to compensate all types of system's errors (due to various factors), independent of their physical nature. However, in practice, industrial robots are equipped with joint encoders only, so the end-effector's absolute location is estimated via the direct kinematic transformation. The absolute measurement systems are usually considered to be expensive and non-suitable for industrial applications; they are mostly used for robotic calibrations or laboratory experiments (Watanabe *et al.* 2006). Typically, such measurement equipment is based on stereo vision systems or laser scanners (Daney *et al.* 2006) that can hardly provide desired data in common industrial environment with numerous obstacles in the neighbourhood of the end-effector.

There are two main components involved in compensation of compliance error; a square matrix (symmetrical or asymmetrical) called Stiffness Matrix that maps the stiffness throughout the working space, the matrix can be defined for both the Cartesian or Joint coordinate system. Other component defines the external loads (linear and angular) acting on the platform during operation of manipulator (in future, it will be referred as loading of manipulator). The stiffness matrix is configuration dependant and differs all over the working space. This work will also contribute to the stiffness matrix computation algorithms.

2.3 Stiffness Modelling of Manipulator

To ensure effective reduction in the compliance errors in machining based on the robots (serial or parallel), a suitable stiffness modelling is required that is capable of considering both

the configuration of manipulator along with the impact of machining forces. In this section, an overview of present available stiffness modelling approaches for parallel, as well as, serial manipulator will be discussed.

2.3.1 Stiffness Modelling and Existing Approaches

In general, like structural mechanics, the stiffness of robots describes the resistivity offered by the manipulator to the distortions produced by external (linear and/or angular) loadings applied at the manipulator (Duffy *et al.* 1996). Numerically, a stiffness matrix [K] is used to define this resistivity property, this matrix defines a relation between the displacements and corresponding loadings that cause the positioning error. The inverse of stiffness matrix [K] is referred to be the compliance matrix which is denoted by [c] or [k] in some literature. For conservative systems, [K] is 6 x 6 positive semi-definite symmetric matrix but it could possess coupling between the linear and angular displacements which can be predicted by off diagonal terms in matrix (Kövecses *et al.* 2007). However, for case of non-conservative systems the stiffness matrix is often asymmetrical.

Due to some specificities, there are few individualities in terminology of stiffness modelling of manipulator. Mostly, the matrix [C K] denotes the "Cartesian Stiffness Matrix" which differs from the "Joint-Space Stiffness Matrix" [θ K] that describes the relation between the static loadings and resulting displacements in both the active and/or passive joints (Ciblak *et al.* 1999). Conservative Congruency Transformation is required to map both the matrices into each other (Kao *et al.* 1999; Chen *et al.* 1999; Huang *et al.* 2002), this transformation is trivial for systems with negligible loadings. However, a complicated equations consisting of the Jacobian, Jacobian derivatives and loading vectors this transformation can become useful (Yi *et al.* 1993).

There are different methods used to find stiffness of hexapod each has its own merits and demerits, main three types are Finite Element Analysis (FEA) famous for its accuracy, Virtual Joint Method (VJM) mostly used for its simplicity and Matrix Structural Analysis (MSA) for its lower computational complexity. Each of three techniques are explained below.

For FEA the body under consideration is divided into small number of elements, these small elements are in standard shapes like; a line (spring) with 2 nodes for 1D element, triangle or square with 3 or 4 nodes for 2D element and pyramid or cube with 4 or 8 nodes for 3D element. The nodes are used for force application and to measure deflection in the body. Each node gives static equilibrium equation by defining a proper relation between nodes, in the form of stiffness matrix. Summation of the stiffness matrix for each node gives global stiffness

matrix. Accuracy of FEA is directly related to the number of divided elements, so analytically FEA is very tedious job and one cannot work beyond certain limits, therefore computational software is required for analysis. Modern FE simulation software is user friendly, the software just need the number of elements in which main body is to be divided (mesh size), the mesh can be further linear for simple analysis or parabolic for highly accurate analysis in which element has more number of nodes than linear mesh. Moreover, the software allows users to view simulations of displacements and deformations of whole body or specific areas of concern that are under stresses. FEA is the most accurate technique often used to verify the results obtained from other techniques like; analytical and experimental (El-Khasawneh *et al.* 1999; Nagai *et al.* 2007; Hu *et al.* 2007; Corradini *et al.* 2003; Li *et al.* 2002; Piras *et al.* 2005) but as the mesh size is refined, higher computational memory is requires also re-meshing is often required with small change in model, so it is time consuming job that is often limited to final stages of design (Huang *et al.* 2002; Pashkevich *et al.* 2011; Long *et al.* 2003).

MSA is another technique which is simplification of FEA, it can be used along with FEA that allows its users to take advantage of the FEA, avoiding high computation for different configuration of body under study, but this can be done only for special cases of unloaded systems (Klimchik 2011). MSA uses element which are larger in size like; beams and arcs, this reduces computational time so results are not as accurate as that of FEA. MSA as main technique was used for stiffness modelling of PM with passive joints and for SP based milling machine (Deblaise *et al.* 2006)(Clinton *et al.* 1997). Working methodology of both the FEA and MSA are almost same, both the methods calculate displacements of nodes of elements under load while working with matrices but from computational side MSA is less complicated than that of FEA. For this technique to work properly, links estimate by beam or arc element should be accurate otherwise results will not be reliable. In short, MSA is special case of FEA which reduces computational time with reasonable accuracy.

VJM is third technique often used in stiffness calculation, body as whole is considered to be rigid but joints liable for flexibility of system. This consideration of flexibility is same as addition of auxiliary virtual joints in real joints using virtual springs. By this lumped representation of stiffness overall model is much simplified than that of considering distributed stiffness in whole system. In (1980), Salisbury applied this method for first time, later C. Gosselin (1990) considered the elasticity source in joints of actuator. His work was further modified to flexible links (Gosselin *et al.* 2002). Defining virtual springs is tough task in itself. In earlier days, each actuated joint was represented by single spring (Zhang 2001; Pigoski, *et al.* 1998; C. M. Gosselin *et al.* 2002). In (2004), Majou *et al.* took flexibility of links by

increasing number of virtual joints in each joint, several virtual springs were introduced in actual joints, in (2007) Majou *et al.* applied VJM for analytical stiffness analysis of parallel manipulator. Most recent development in VJM is taking 6 DOF virtual springs to replace link's flexibility (Pashkevich, *et al.* 2009). The increase in number of springs made VJM as good as FEA with additional advantage of lower computational costs. VJM is not suited for stiffness modelling of parallel manipulators because of sequential chains between the base plate and platform, for such internal looped structures defining VJM based stiffness analysis becomes complicated.

2.3.2 Computational Complexity.

The computational complexity of any of the method described above can be estimated by the computational resources required for inversion of matrices in algorithm. The computational complexity required for calculation of matrix of order *nxn* is $O(n^3)$ which is calculated by Lin *et al.* (2011), where "O" represents orthogonal matrix group.

For the FEA method *n* in $O(n^3)$ depends on two things; the mesh size of element and the nature of mesh elements (linear or parabolic). For parabolic shaped mesh there are 12 connections in 10 nodes between each element. The value of *n* changes to $30vn_L$, where n_L is the number of links of manipulator and v represents mesh size per element (v must be atleast 103 for reliable results).

For case of MSA analysis, "n=12 n_d" representing the upper bound of the matrix size which is computed using the node number n_d. For VJM method, the matrix to be inverted has size n= 6+ n_q; where n*q* is the number of the DOF of spring with which the passive joints are represented.

The computational complexity of each method calculated by Klimchik (2011) is presented in table 2-1. From the Klimchik's study it can be concluded that the VJM is least complex method and FEA is about five time more complex than VJM, MSA stands in between both methods.

Table: 2-1 Complexity while solving Stiffness model; (Klimchik 2011)

Stiffness modelling method	Complexity of Stewart platform
FEA	$\sim 10^{16}$
MSA	$\sim 10^{6}$
VJM	$\sim 10^{3}$

2.3.3 Stewart Platform and its Stiffness:

Stewart Platform is six DOF hexapod, which was originally used for flight simulation by Stewart. The platform was hexapod with a fixed plate connected by six legs having prismatic joint in centre, furthermore, a spherical and a revolute joint was attached at upper and lower ends of each leg at fixed and movable platform, respectively (Stewart 1965). Stewart utilized the same idea that was used by Gough in late 1940s for his universal tyre testing machine figure 2-4, but published in 1962 (Gough *et al.* 1962), so in some literature it is referred as Gough Stewart Platform (GSP). Nowadays, SP is being used in different machining processes for higher precision and rigidity (Clinton *et al.* 1997). Different changes in SP were made to improve its performance like; SP with improved dexterity was presented by Stoughton *et al,* (1993) the work was named as Modified SP, figure 2-5; struts were connected in two

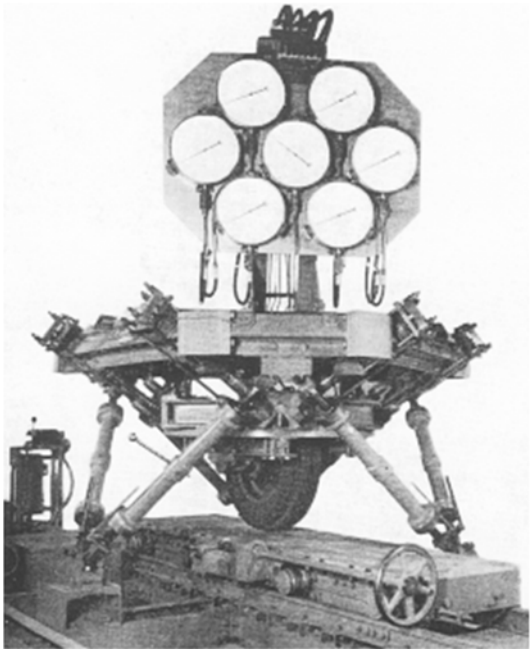

Figure: 2.4 Gough Universal Tyre Testing Machine (Gough *et al.* 1962)

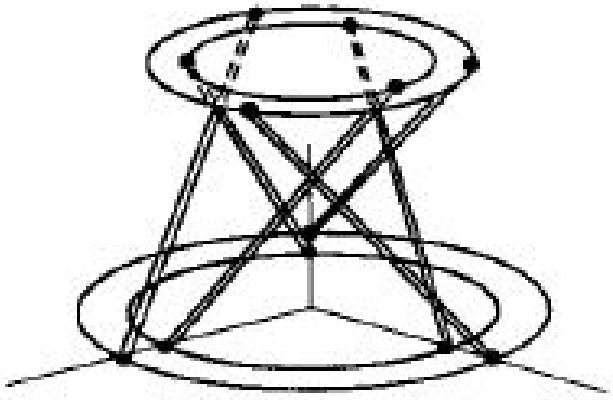

Figure: 2.5 Modified Stewart Platform (Stoughton *et al.* 1993)

circles instead of single circle, result was about 30% improvement in force and torque than that of SP proposed by Stewart, however, this change in arrangement of legs reduced the workspace of platform (Stoughton *et al.* 1993). Performance of system greatly rely on its stiffness, as stiffness is the ability of a system to withstand forces without extreme deformations in its structure, so accuracy and position of end effector highly depends on stiffness of system. Stiffness determines deformation of system under applied load, also the positional accuracy is directly related to stiffness (Portman *et al.* 2000).

Stiffness attracted attention of many researchers. A relationship between Lagrangian and Cartesian stiffness matrix for PM with elastic joints and rigid links is defined using principle of virtual work (Ruggiu *et al.* 2012). Stiffness of PM is focused by Huang *et al.* (2002) using principle of superposition; whole system is divided into two parts machine frame and parallel mechanism while studying the machine frame the parallel mechanism is kept rigid and vice versa. The superposition is applied to find stiffness as a whole (Huang *et al.* 2002). In (1999), El-Khasawneh *et al.* calculated stiffness of SP using inverse kinematics and Jacobian of manipulator, as the stiffness of platform is direction dependant so stiffness of PM in particular directions is discussed. In their work maximum and minimum bounds of stiffness are also developed.

In (1993), Lebret *et al.* studied the dynamics and applications of SP in manufacturing industry using Lagrange's formulation. Lagrange formulation was also used by Butt *et al.* in (Butt *et al.* 2013) to calculate positional error in rigid baseplate during precise machining of precious metal used in hip prosthesis The position error was due to elastic locators with elastic contacts configuration. Hernez *et al.* in (2014) focused on the errors in legs of SP that occurred due to manufacturing issues, a numerical methodology is formulated that compensates the displacement errors and simulates its effects in histogram but the proposed approach is only applicable on systems having error data in pattern. Nagai *et al.* in (2007) proposed a systematic approach to calculate stiffness by considering both the joints and the links as flexible elements, the proposed systematic approach has set of rules; passive forces are temporarily assumed to be non-zero, certain links are either fixed or joined to passive joints, for validation the proposed approach is applied on 2 DOF PM with passive joints and eventually applied on NINJA to find its overall stiffness.

Position error caused due to deformation of links and joints in presence of external forces is calculated by Ahmad *et al.* (2014), their work consists of two parts; a simple model and a detailed model, in simplified model only links are deformed due to applied forces and moments, summation of stiffness of each leg gives global stiffness matrix, results are iteratively

compared with FEA results with small model parameter adjustments when both results are validated, an experiment is carried out for same model. In case simplified modelling is failed, a detailed modelling is carried out in which flexibility of joints and actuators are also considered and whole processes is repeated again, by comparison of both the simplified and detailed models it is concluded that by considering flexibility of joints and actuators, the average error between experiments results and analytical results can be reduced from 80% to 9%.

Carbone (2011) worked on stiffness calculation of multi body robotic system using both the analytical as well as experimental techniques, to save computational time lumped parameter model was used instead of FEA, stiffness properties of both the links and the actuators were taken into account using linear and torsion springs. In (2005), Piras *et al.* derived linear dynamic model of moving mechanisms while considering flexibility in links, both the linear and transverse directions of links were taken into account to study flexibility of links, moreover, linear actuators were also included in proposed mathematical model, a FE simulation was also performed for validation and it was concluded that high speed motion deflection of mechanism depends on its configuration.

In (2009), Pashkevich *et al.*, considered flexibility of links and focused on non-linear analysis of stiffness of modulator to present methodology that enables study of buckling deflection with other non-linear phenomenon for elastic behaviour of manipulator under applied machining forces, the proposed model was based on multi-dimensional lumped parameter. Bhattacharya *et al.* (1995) used nonlinear techniques to study rigidity behaviour of PM considering elastic legs under axial loading, finally nonlinear optimization techniques were applied to find optimum design parameters for Hexapod. Other objective of the work includes formulation of a scalar to measure rigidity of SP type PM to obtain most rigid design, this was done using multi objective optimization technique in which two design parameters were (1) arrangement angle "α" of leg at upper platform and (2) ratio of radius of two plates, with "α"=0 platform was at its maximum rigidity.

Afzali-Far *et al.* (2014), proposed analytical model that includes study of inertia, damping, flexibility of struts in axial direction and stiffness matrix, Lagrange equation and Bryant angles are used for mathematical model development, the proposed model is developed in term of twelve design variables with neutral configuration of platform so it can be used for design and optimization of any SP, they also used Eigen values and frequencies in Cartesian space.

For stability of any structure in working environment its Eigen values and natural frequencies play leading role, Eigen values and natural frequencies are important part of many research works. In (2009), Mahboubkhah *et al.* presented a study in which free vibrations of hexapod table of machine tool were investigated, it consisted of two different techniques, (1) all kinematics chains of hexapod were involved in evaluation of coupled system of equations and (2) vibration equation of moving platform were derived considering flexibility as well as damping of supporting chains.

2.4 Conclusion

Although much work had been done on stiffness analysis yet there is research gap of finding the way in which stiffness from different techniques like analytical, experimental and FEA yields same result (Carbone 2011). This mismatching of results could be due to several reasons like; by ignoring friction forces, force due to gravity or any surrounding disturbance which is present during experiments but overlooked during simulation, another reason could be modelling of 3D systems in 1D or 2D systems. We observed in literature that there is almost always small deviation between experimental, simulation and analytical results (El-Khasawneh *et al.* 1999; Ahmad *et al.* 2014; Huang *et al.* 2002; Clinton *et al.* 1997). This is because often simulations or analytical work is 1D or 2D while experimental work is always in 3D, which causes some error.

In the present work, it is proposed to calculate the stiffness matrix for Stewart platform by considering each leg of platform as 3D elastic truss. Analytical model is used for the calculation of the overall energy of the system. Lagrangian formulation is utilized to calculate the displacements of the upper platform of hexapod under external loadings. A generic algorithm is formulated in MATHEMATICA®, which calculates stiffness of "n" legged PM. Stewart platform with same dimensions is modelled and simulated in CATIA® to validate proposed methodology. This work is an effort in minimizing computational time for predicting the workpiece displacement under the working condition.

CHAPTER 3: METHODOLOGY

In this chapter methodology of proposed work will be explained. It includes the calculation of potential energy of each leg by considering each leg to be a 3D massless elastic truss and the calculation of total work done due to external machining forces on the platform. This methodology is proposed while keeping in mind the structure of Stewart Platform but is applicable to all parallel manipulator family of Group 1[1]. In the end, kinetic energy of platform due to its mass and machining forces is studied to calculate the Eigen value and Eigen vector of the platform.

3.1 Mechanical Model Representation

The basic representation of system, modelled in CATIA, without external forces is shown in figure 3-1. During the mechanical modelling, the legs are taken as massless 3D elastic trusses, each leg is represented by proper stiffness matrix *[(K1) to (K6)]*. The platform is assumed to be a rigid mass element i.e. no deformation is possible under machining forces. The spherical contacts of legs are also assumed to be rigid so no deformation modelling is established between the plates and legs of the system. Aim of this mechanical model is to calculate the displacements of "platform" due to external forces, along, with 3D Stiffness matrix of the system due to elasticity of legs. Using the calculated Stiffness matrix, Eigen values and their corresponding Eigen vector are also calculated.

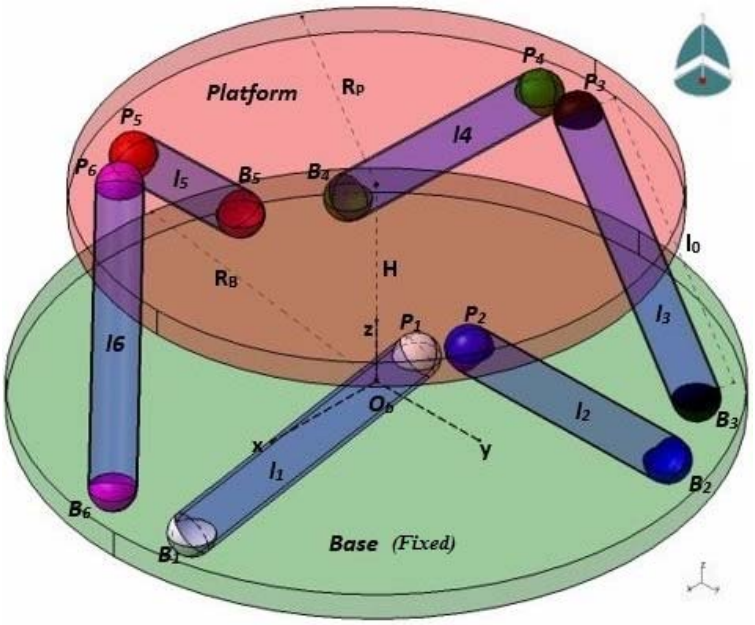

Figure: 3.1 Isometric view of Stewart Platform Model

[1] Categorised in Chapter 1

The term arrangement angle of the legs at lower and upper plates shows the placement angles of legs at corresponding plate. To make a truss structure for stability of system, axis at base plate is taken at *0˚*, however, axis for platform are initially rotated at angle of *60˚* and for symmetry of system each leg at base is placed at angle of *10˚* (θ_B) and *6˚* (θ_P) at platform as shown in figure 3-2.

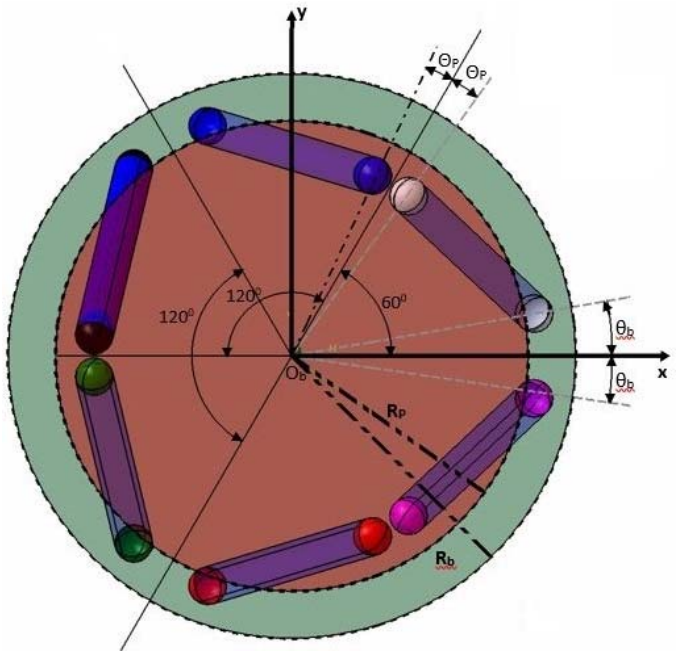

Figure: 3.2 Top view of Stewart Platform Model

3.2 Positioning error due to deformation of elastic legs

The legs of manipulator can deform either under the weight of the platform or due to dynamic (machining) forces exerted on the platform by the tool. The displacements as the result of external forces are required to calculate the positioning error of platform.

In this section, an analytical model is proposed that calculates the deformation of elastic legs due to displacement of the rigid platform under external load. This analytical model will be referred as "mechanical model" in report. The proposed model calculates the stiffness of elastic legs and mass of the upper platform, the legs are assumed to be the 3D trusses with negligible masses and the platform of system will be the rigid massed body.

As the FEA method needs tedious initial modelling of the system whenever the configuration or condition of the system changes. Therefore, the analytical formulation is preferred for the solution of this problem. The proposed methodology will allow to obtain the mass matrix, stiffness matrix and displacements of upper platform quickly for any configuration, as well as, for any initial orientation of the parallel manipulator, the inputs are introduced by just editing the input spreadsheet file, generated by Mathematica®.

The Lagrangian formulation is programmed in Mathematica® to obtain the stiffness matrix. The calculated matrix depends on the configuration of platform and changes with alternations in the design parameters like; platform's initial orientation, dimensions and material properties, etc. Small displacement approximation is used as the deformation must remain small for precision of the system.

Followings will be the main focuses of the chapter: in start, the proposed analytical model was constructed assuming the platform being rigid with elastic legs. Later, the overall energies of the system are obtained, these energies include the potential energies of all the legs of system, kinetic energy of inertial elements (platform) and overall work done due to the machining loads acting on the platform. Lagrange equation takes the KE, PE and work done as inputs and calculates the displacement of platform, furthermore, Hessian of the calculated PE gives stiffness matrix and KE gives mass matrix of the platform, these matrices are used for calculation of Natural Frequencies and mode shapes of the platform. During the calculations, it is assumed that the contacts between the legs, the base, as well as, the platform are rigid.

3.3 Mechanical Behaviour Formulation

In this section, the mechanical behaviour of the system is formulated using Lagrange formulation and assuming small displacement approximation. The general Lagrange equation is given below;

$$\frac{\partial}{\partial t}\left(\frac{\partial(KE-PE)}{\partial \dot{q}_i}\right)-\frac{\partial(KE-PE)}{\partial q_i}-\frac{\partial W}{\partial q_i}=0 \tag{3.1}$$

where, PE is the total potential energy of all the elastic bodies in the hexapod, KE represents total kinetic energy of inertial parts, W represents work that is done by external machining forces and torques on the platform, q_is represent generalized coordinate. For this study, q_i's are the 6-DOF and $\dot{q}_i$ represents six velocities ($q_i = \left(\frac{\partial q_i}{\partial t}\right)$) of the system.

The external forces may relocate the workpiece, however, to simplify the model it is supposed that the machining forces are directly applied on rigid platform so no displacement can take place between the platform and workpiece under load or work piece is also taken as a rigid body.

Main aim of upcoming sub-sections is to estimate the displacement produced in the platform under machining forces which is the relative to the initial position of the platform to that of unloaded. This displacement of platform is the positioning error of the platform. The information of the system's configuration consists of; initial orientation of platform, material

property, dimensions of system along with the magnitude and direction of the applied machining forces and moments. The stiffness and mass matrices are calculated assuming small displacements and Lagrangian formulation.

3.3.1 Calculation of Leg Length

The calculation of the length of leg requires its coordinates at the platform and the base. The lower coordinates are calculated using radius of base plate and arrangement angles of leg on the base, as the origin is assumed at the upper face of base therefore in z-axis will be "0", lower coordinates can be calculated using equation (3.2). Similarly, for leg's coordinate at the platform, leg's arrangement angles at platform and radius of platform are required, in this case z axis will have value same as that of point "P", equation (3.3).

$$Lower\ coordinates\ = \begin{pmatrix} Radius\ of\ lower\ *\ cos\,\theta \\ Radius\ of\ lower\ *\ sin\,\theta \\ 0 \end{pmatrix} \tag{3.2}$$

$$Upper\ coordinates\ = \begin{pmatrix} Radius\ of\ upper\ *\ cos\,\theta \\ Radius\ of\ upper\ *\ sin\,\theta \\ Z\ zxis\ of\ "P" \end{pmatrix} \tag{3.3}$$

If there is any initial orientation of platform, it must be introduced in this step by pre-multiplication of RPY[1] rotation matrix with upper coordinates of legs. This multiplication will change the length of certain legs according to rotation matrix. Hence, the platform will get an initial orientation in local coordinates using equation 3.4, which is converted into global coordinates using equation 3.5.

$$Rotated\ Upper\ coordinates = \begin{bmatrix} 1 & -\Delta\alpha & \Delta\gamma \\ \Delta\alpha & 1 & -\Delta\beta \\ -\Delta\gamma & \Delta\beta & 1 \end{bmatrix} . \begin{bmatrix} Radius\ of\ upper\ *\ cos\,\theta \\ Radius\ of\ upper\ *\ sin\,\theta \\ 0 \end{bmatrix} \tag{3.4}$$

$$Final\ Upper\ coordinates = Rotated\ Upper\ coordinates + \begin{bmatrix} 0 \\ 0 \\ Z\ axis\ of\ "P" \end{bmatrix} \tag{3.5}$$

Now, using two coordinates of each leg, the calculated points can be used for calculation of length of leg using distance formula which is given as

$$Leg\ length = \sqrt{(x_L - x_U)^2 + (y_L - y_U)^2 + (z_L - z_U)^2} \tag{3.6}$$

where x_L, y_L, z_L and x_U, y_U, z_U are lower and upper coordinates of leg, respectively.

(Dukkipati *et al.* 2012), used the components of the unit vector calculated form length of each leg, these components are used form calculation of 3D Stiffness matrix of each leg,

[1] YRP: Yaw (α) Roll(β) Pitch(γ)

summation of which can be used for calculation of global potential energy of the system with massless elastic legs.

3.3.2 Elastic Potential Energy

Consider again, the hexapod shown in figure 3-1, overall PE of this hexapod is summation of individual PE each leg possesses, the only elastic body in the system, besides, whole assembly is assumed to be rigid. Each leg is assumed to 3D elastic truss. The overall potential energy of the i^{th} elastic legs is given by;

$$PE_i = {}^1/_2 \ \{\Delta X\}_i \ [K]_i \ \{\Delta X\}_i^T \tag{3.7}$$

$$\{\Delta X\} = \{0 \quad 0 \quad 0 \quad \Delta X_i \quad \Delta Y_i \quad \Delta Z_i\}$$

where, $[K]_i$ represents stiffness matrix for i^{th} leg

$\Delta X_i, \Delta Y_i, \Delta Z_i$ are components of displacement vector, the displacements of the point of contact of i^{th} leg attached to upper plate

ΔX_i represents displacement of the point of contact of i^{th} leg due to its elasticity, Dukkipati *et al.* (2012) defined stiffness matrix for 3D truss body as :

$$K = {}^{AE}/_L \begin{bmatrix} k' & -k' \\ -k' & k' \end{bmatrix} \tag{3.8}$$

$$\text{where, } k' = \begin{bmatrix} \lambda_x^2 & \lambda_x\lambda_y & \lambda_x\lambda_z \\ \lambda_y\lambda_x & \lambda_y^2 & \lambda_y\lambda_z \\ \lambda_z\lambda_x & \lambda_z\lambda_y & \lambda_z^2 \end{bmatrix}$$

λ_x, λ_y, λ_z are i^{th}, j^{th} and k^{th} components of unit vector of length of leg obtained by leg's point of contact at the platform and base plate.

An imaginary point "P" is chosen with respect to which the displacement vector is measured, any arbitrary point could be chosen for this purpose, however, for this study, this point is the centre of gravity of the platform. If α, β and γ are three rotations for the platform in Cartesian coordinates, the location of i^{th} point of contact on the platform, w.r.t. arbitrary point "P", is defined as;

$$\begin{bmatrix} x_{fi} \\ y_{fi} \\ z_{fi} \\ 1 \end{bmatrix} = \begin{bmatrix} cos\alpha\ cos\gamma - sin\alpha\ sin\beta\ sin\gamma & -sin\alpha\ cos\beta & cos\alpha\ sin\gamma - sin\alpha\ sin\beta\ cos\gamma & Xp \\ sin\alpha\ cos\gamma + cos\alpha\ sin\beta\ sin\gamma & cos\alpha\ cos\beta & sin\alpha\ sin\gamma - cos\alpha\ sin\beta\ cos\gamma & Yp \\ -cos\beta\ sin\gamma & sin\beta & cos\beta\ cos\gamma & Zp \\ 0 & 0 & 0 & 1 \end{bmatrix} \begin{bmatrix} x_i - x_p \\ y_i - y_p \\ z_i - z_p \\ 1 \end{bmatrix} \tag{3.9}$$

where, $x_i - x_P$, $y_i - y_P$, and $z_i - x_P$, represents the position vector between the initial contact point and chosen imaginary point "P", x_{fi}, y_{fi} and z_{fi} shows final position of i^{th} point after its displacement, and X_P, Y_P and Z_P represents the displacements of imaginary point of the platform under external forces. According to small displacement assumption:

$\sin\theta \approx \theta$, $\cos\theta \approx 1$

$\sin\theta \cos\theta \approx 0$

$\sin^2\theta \approx 0$

After applying the small angles hypothesis, the equation 3.9, is reduced to;

$$\begin{bmatrix} x_{fi} \\ y_{fi} \\ z_{fi} \\ 1 \end{bmatrix} = \begin{bmatrix} 1 & -\Delta\alpha & \Delta\gamma & \Delta X_P \\ \Delta\alpha & 1 & -\Delta\beta & \Delta Y_P \\ -\Delta\gamma & \Delta\beta & 1 & \Delta Z_P \\ 0 & 0 & 0 & 1 \end{bmatrix} \begin{bmatrix} x_i - x_p \\ y_i - y_p \\ z_i - z_p \\ 1 \end{bmatrix} * \tag{3.10}$$

The final coordinates of i^{th} point w.r.t. point P, after displacement, is obtained by subtraction of the final position of contact point from its initial position w.r.t. "P" on the platform. The final position of i^{th} point of contact becomes;

$$\begin{bmatrix} \Delta X_i \\ \Delta Y_i \\ \Delta Z_i \\ 1 \end{bmatrix} = \begin{bmatrix} 0 & -\Delta\alpha & \Delta\gamma & \Delta X_P \\ \Delta\alpha & 0 & -\Delta\beta & \Delta Y_P \\ -\Delta\gamma & \Delta\beta & 0 & \Delta Z_P \\ 0 & 0 & 0 & 1 \end{bmatrix} \begin{bmatrix} x_i - x_P \\ y_i - y_P \\ z_i - z_P \\ 1 \end{bmatrix} * \tag{3.11}$$

Equation 3.11 enables us to calculate the deformation of each leg's contact point which leads to the calculation of potential energy of massless elastic legs as the function of six unknowns (linear and angular) displacements of the platform $\{\Delta X_P, \Delta Y_P, \Delta Z_P, \Delta\beta, \Delta\gamma, \Delta\alpha\}^T$.

3.3.3 Inertial Kinetic Energy

The system under study is supposed to be at static configuration so its velocity is zero, hence kinetic energy will be zero. But there will be small kinetic energy due to mass of platform, the only inertial body in the system, it will experience kinetic energy due to external machining loads. Kinetic energy consists of; linear and angular kinetic energies. The general equation for linear kinetic energy (T_V) is given as;

$$T_V = \frac{1}{2}\{\vec{V}\}\,[M]\,\{\vec{V}\}^T \tag{3.12}$$

where M is consistent mass matrix of platform, $\{\vec{V}\}$ is linear velocity vector with components;

$$\vec{v}_x = \frac{\delta X_p}{\delta t}, \vec{v}_y = \frac{\delta Y_p}{\delta t}, \quad \vec{v}_z = \frac{\delta Z_p}{\delta t} \tag{3.13}$$

$M = \rho\pi H(R_P)^2$

The equation 3.12 gives the linear velocity vector in terms of six unknown displacements of the platform. Similarly, the angular kinetic energy in term of unknown variables is calculated using equation 3.14.

$$T_\Omega = \{\vec{\Omega}\}\,[I]\,\{\vec{\Omega}\}^T \tag{3.14}$$

where [I] is the inertia matrix

$$[I] = \begin{bmatrix} \frac{1}{12mh^2} + \frac{1}{4}mr^2 & 0 & 0 \\ 0 & \frac{1}{12mh^2} + \frac{1}{4}mr^2 & 0 \\ 0 & 0 & \frac{1}{2}m\,r^2 \end{bmatrix} \quad (3.15)$$

and $\{\vec{\Omega}\}^T = \{\vec{\omega_x}, \vec{\omega_y}, \vec{\omega_z}\}$ is the angular velocity vector. Lalanne *et al.* (1986), calculated angular velocities, figure 3-3 shows the platform that bears three rotations α, β and γ about z, x and y axis, respectively. Angular velocities calculated by Lalanne *et al.* (1986) are function of three angular displacements, these velocities are given as,

$$\vec{\omega}_x = -\frac{\delta\alpha}{\delta t}cos\beta sin\gamma + \frac{\delta\beta}{\delta t}cos\gamma \quad (3.16a)$$

$$\vec{\omega}_y = -\frac{\delta\gamma}{\delta t} + \frac{\delta\alpha}{\delta t}sin\beta \quad (3.16b)$$

$$\vec{\omega}_z = -\frac{\delta\alpha}{\delta t}cos\beta cos\gamma + \frac{\delta\beta}{\delta t}sin\gamma \quad (3.16c)$$

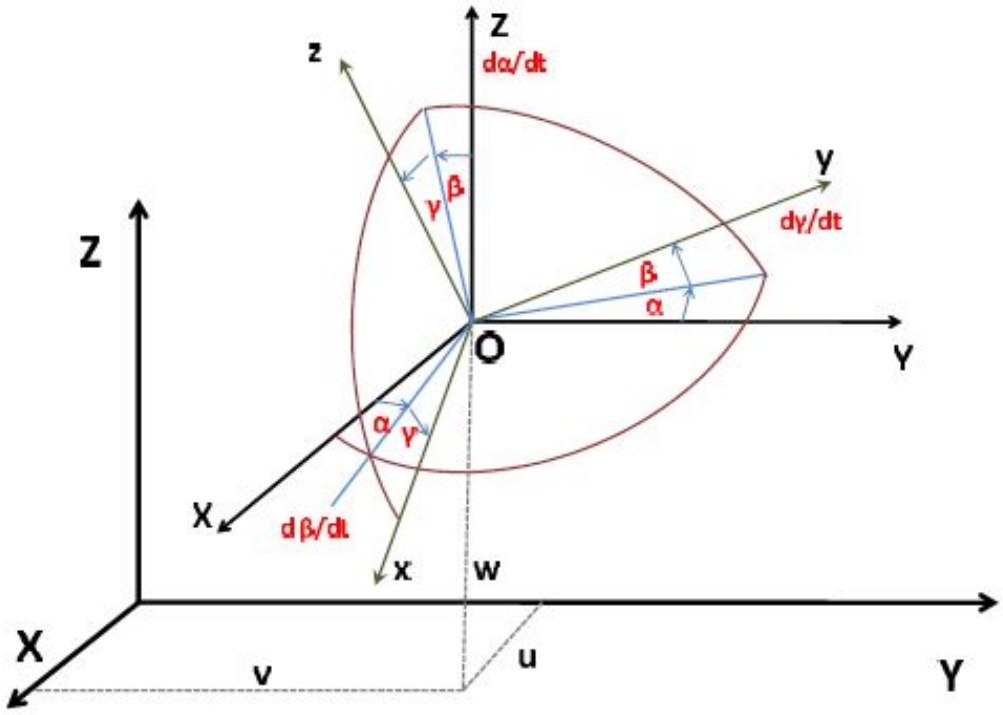

Figure: 3.3 Rotation along axis [β, γ and α about x, y and z axis](Lalanne *et al.* 1986)

The small angle displacement hypothesis $\cos\theta \approx 1, \sin\theta \approx \theta$ reduces equation 3.16 to equation 3.17

$$\vec{\omega}_x = -\frac{\delta\alpha}{\delta t}\gamma + \frac{\delta\beta}{\delta t} \quad (3.17a)$$

$$\vec{\omega}_y = -\frac{\delta\gamma}{\delta t} + \frac{\delta\alpha}{\delta t}\beta \quad (3.17b)$$

$$\vec{\omega}_z = -\frac{\delta\alpha}{\delta t} + \frac{\delta\beta}{\delta t}\gamma \quad (3.17c)$$

Equations 3.12 and 3.14, calculate both the linear and angular KE of the platform as a function of six unknown displacements $\{\Delta X_P, \Delta Y_P, \Delta Z_P, \Delta\beta, \Delta\gamma, \Delta\alpha\}^T$. Hence, like potential energy, kinetic energy will also be calculated as a function of unknown displacements of the platform. Summation of linear and angular kinetic energies will give us total kinetic energy of the platform:

$$T = T_V + T_\Omega \tag{3.18}$$

In this thesis, the kinetic energy is neglected but it is of great importance in turning process.

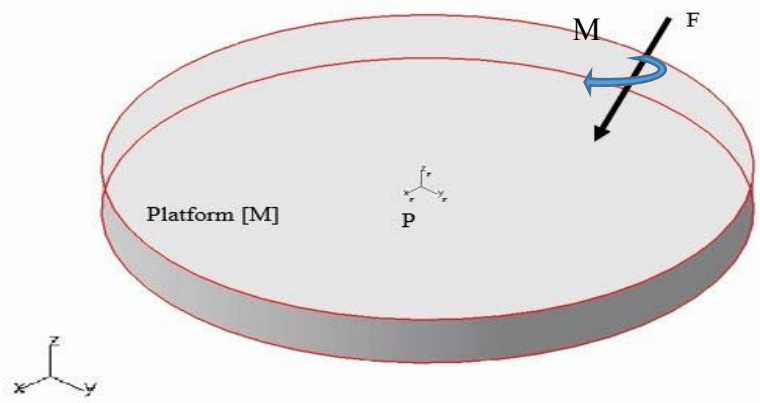

Figure: 3.4 Platform with machining force

3.3.4 Total Work done by External Forces

The forces applied by the machining tool (linear and moment) on platform are treated as the external forces. In this section, total work done by the machining tool will be calculated. In figure 3-4, the platform is shown without legs and is experiencing a point machining load F = $\{Fx, Fy, Fz\}^T$ with moment M = $\{Mx, My, Mz\}^T$. For the machining force acting at point other than point "P", there will be some angular displacement along with linear displacement of the platform. Total work done the static force is calculated in equation 3.19.

$$W = \{F\}.\{\Delta X_P\} + \{M\}.\{\Delta\theta\}^* \tag{3.19}$$

where, F represents linear force, ΔX_P shows linear displacements of point P under force F, T is the torque applied by the tool with $\Delta\theta$ resultant angular displacement vector. 3D view of the platform is shown in figure 3-5, with a force and moment component.

There is some displacement of point of action of force due to mutual effect of elasticity of legs and applied force. The displacement of the point of application of force can be written as the function of 6 DOF of the platform as shown in equation 3.20 using small displacement approximation as;

$$\begin{Bmatrix} \Delta X_{pf} \\ \Delta Y_{pf} \\ \Delta Z_{pf} \\ 1 \end{Bmatrix} = \begin{bmatrix} 0 & -\Delta\alpha & \Delta\gamma & \Delta X_P \\ \Delta\alpha & 0 & -\Delta\beta & \Delta Y_P \\ -\Delta\gamma & \Delta\beta & 0 & \Delta Z_P \\ 0 & 0 & 0 & 1 \end{bmatrix} \begin{Bmatrix} x_f - x_P \\ y_f - y_P \\ z_f - z_P \\ 1 \end{Bmatrix} * \tag{3.20}$$

where, $\{x_f - x_P, y_f - y_P, z_f - z_P\}$ shows the position vector between application point of

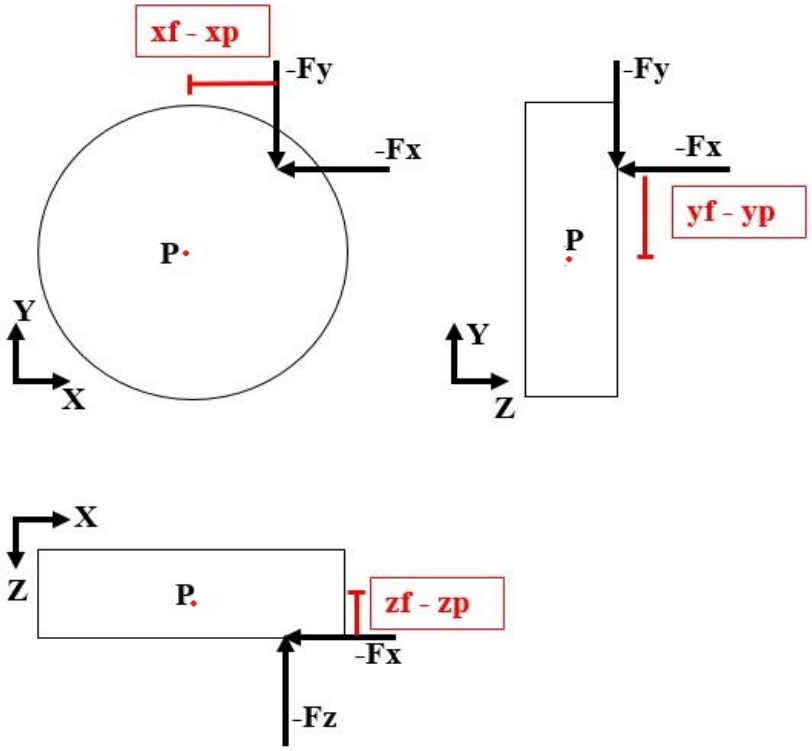

Figure: 3.5 Three views of Platform with machining force

force w.r.t. imaginary point, while $\{\Delta X_{Pf}\} = \{\Delta X_{Pf}, \Delta Y_{Pf}, \Delta Z_{Pf}\}$ is the displacement of point at which the force (F) is applied, like KE it is also in term of six unknown displacements $\{\Delta X_P, \Delta Y_P, \Delta Z_P, \beta, \Delta\gamma, \Delta\alpha\}$ of the platform. For "i" forces and "j" moments equation 3.21 becomes;

$$W = \sum_{i=1}^{n} \left[\begin{Bmatrix} F_x \\ F_y \\ F_z \end{Bmatrix}_i . \begin{Bmatrix} \Delta X_f \\ \Delta Y_f \\ \Delta Z_f \end{Bmatrix}_i \right] + \sum_{j=1}^{n} \left[\begin{Bmatrix} M_x \\ M_y \\ M_z \end{Bmatrix}_j . \begin{Bmatrix} \Delta\beta \\ \Delta\gamma \\ \Delta\alpha \end{Bmatrix}_j \right] \tag{3.21}$$

where, $\{\Delta X_f, \Delta Y_f, \Delta Z_f\}$ represents linear displacement vector and $\{\Delta\beta, \Delta\gamma, \Delta\alpha\}$ shows angular displacement vector of the platform. Using calculated equations for the potential energies of legs, kinetic energy of the platform and work done by the machining loads, the Lagrange equation (equation. 3.1) uses calculated KE, PE and work done to find the stiffness matrix, mass matrix, six unknown displacements of the platform under machining forces, using the mass and stiffness matrices the natural frequencies of the hexapod can be investigated.

3.3.5 Displacement of platform under load

Major focus of this work includes computation of the positioning error of the platform under the forces exerted by machining tool, the machining forces are directly acting on the rigid platform which is mounted on the elastic legs with rigid joints. The total energies of system (KE and PE) and the work done by all the machining loads (linear and angular) are explained in previous sections. All calculated terms are function of six unknown variables $\{\Delta X_P, \Delta Y_P, \Delta Z_P, \Delta\beta, \Delta\gamma, \Delta\alpha\}$. The calculated energy terms with Lagrange equation (equation 3.1) gives the displacement vector of the platform. There will be separate equation for each leg, so for "n" legs algorithm will generate "n" linear equations. The statically determinate problem will be solved for six unknown displacements. To obtain the unknowns this algorithm is programmed in Mathematica assuming small displacement approximation, i.e.

$$\dot{q}_i \approx 0, \ddot{q}_i \approx 0, q_i q_j \approx 0$$

where, q_is represent the 6 DOF parameters (ΔX_P, ΔY_P, ΔZ_P, $\Delta\beta$, $\Delta\gamma$, $\Delta\alpha$) of the workpiece, $\dot{q}_i$ represents the velocity parameters with $\dot{q}_i = \frac{\delta q_i}{\delta t}$ and $\ddot{q}_i$ represents the acceleration parameters with $\ddot{q}_i = \frac{\delta^2 q_i}{\delta t^2}$ of the considered system.

3.3.6 Natural Frequencies of the System

The mechanical behaviour of the hexapod can also be studied using potential and kinetic energies. Mass matrix is obtained from the calculated Kinetic energy, similarly, the global stiffness matrix is obtained from the overall PE of the system, as shown in figure 3-6. From equation 2.2 and equation 2.13, the component i × j of the stiffness and mass matrices are obtained using equation. 3.22a and equation. 3.22b.

$$[Kij] = \frac{\delta U}{\delta qi \delta qj} \quad (3.22a)$$

$$[Mij] = \frac{\delta T}{\delta \dot{q}i \delta \dot{q}j} \quad (3.22b)$$

Using calculated stiffness matrix of legs and mass matrix of platform, the Natural frequencies and mode of the system can be analysed using the equation 2.18, (Dukkipati *et al.* 2012) gives this equation as;

$$|[M]^{-1}[K] - \omega^2[I]| = 0 \quad (3.23)$$

The natural frequency determines the safe operating frequency of the platform. For safety, the frequency of the machine tool should be different from the natural frequencies of the hexapod.

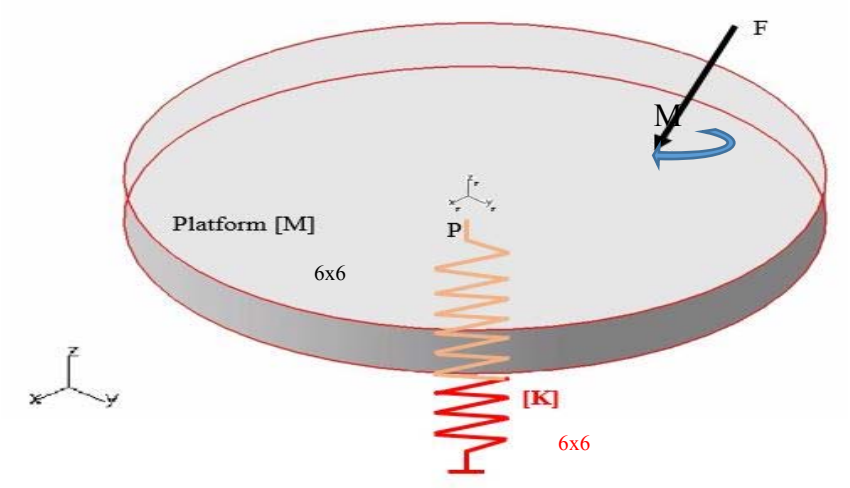

Figure: 3.6 Overall stiffness and Mass matrix representation

3.3.7 Displacement of Any Point on Platform

The calculation described in above sections is for Point "P", the centre of gravity of platform, however, linear displacement of any point on the platform can be calculated by multiplying the HTM[1] with a position vector form point "P" to the point of interest, whose linear displacement is required. The displacement of any point other than "P" can be calculated using equation. 3.24.

$$\begin{bmatrix} \Delta X_O \\ \Delta Y_O \\ \Delta Z_O \\ 1 \end{bmatrix} = \begin{bmatrix} 0 & -\Delta\alpha_P & \Delta\gamma_P & \Delta X_P \\ \Delta\alpha & 0 & -\Delta\beta_P & \Delta Y_P \\ -\Delta\gamma & \Delta\beta_P & 0 & \Delta Z_P \\ 0 & 0 & 0 & 1 \end{bmatrix} \begin{bmatrix} x_O - x_P \\ y_O - y_P \\ z_O - z_P \\ 1 \end{bmatrix} \quad (3.24)$$

where; $\{\Delta\alpha_P, \Delta\beta_P, \Delta\gamma_P, \Delta X_P, \Delta Y_P, \Delta Z_P\}$ are six displacements calculated by Lagrangian formulation

$\Delta X_O, \Delta Y_O, \Delta Z_O$ are displacements of the point of interest on the platform

x_O, y_O, z_O, are the coordinates of any other point of interest

x_P, y_P, z_P, are the coordinates of point "P", with reference to which displacements of platform are calculated. It should be noted that equation 3.24 is used for validation of angular displacement in next chapter.

3.4 Conclusion

This chapter was devoted to establishment of a mechanical model of the hexapod to compute the displacement error of the platform and its behaviour under machining forces and in environment, respectively. To do this, stiffness and mass matrices of the "n" legged hexapod

[1] Homogenous Transformation Matrix

are calculated assuming the legs to be 3D massless elastic trusses keeping the platform assembly as rigid mass body with rigid spherical contacts with legs. Using the proposed analytical methodology, stiffness matrix for any initial configuration and orientation of the platform can be accurately estimated. The methodology is modelled in Mathematica®. To make the algorithm reliable, the deformation must remain small, so small displacement hypothesis is used.

The proposed mechanical model of hexapod is demonstrated by considering platform and joints being rigid with elastic legs. Total energy of the hexapod is computed, the energy constitutes of the potential energy within all elastic legs, kinetic energy due to mass of platform and work done by all the machining forces applied on the platform. Solution of Lagrange equation gives; displacement of the platform under external loading, the stiffness and mass matrices along with vibrational behaviour of the platform, deformation of each leg depends on the stiffness matrix of leg. During the evaluation, contacts between the legs and platform and the platform itself is kept rigid. The proposed methodology is capable of solving complex problems with different number of machining forces and with different initial orientation of platform.

CHAPTER 4: CASE STUDY AND FE ANALYSIS

In this chapter, a case study is performed on a Stewart platform, designed and developed by Physik Instrumente, model H-840 ("H-840 6-Axis Hexapod" 2016), shown in figure 3-1, to explain the working and findings of the proposed mechanical model. It has repeatability of $\pm 0.4\mu m$ and resolution of *16nm*, H-840 with same specification as provided by its manufacturers (table 4-1), is designed in CATIA (figure 4-2) to evaluated the displacement of platform and natural frequencies of the system. Force "F" is taken as machining force at any point on the platform, the model is capable to take into account the effect of "n" forces, *[K1]* to *[K6]* are stiffness matrices of legs (1 to 6) that are taken to be 3D trusses.

Figure: 4.1 PI H-840 Hexapod

Table: 4-1 Specifications of Hexapod

Symbol	Value	Symbol	Value
R_b	0.130m	H	0.085m
R_p	0.105m	θ_p	6^0
r	0.01m	θ_b	10^0

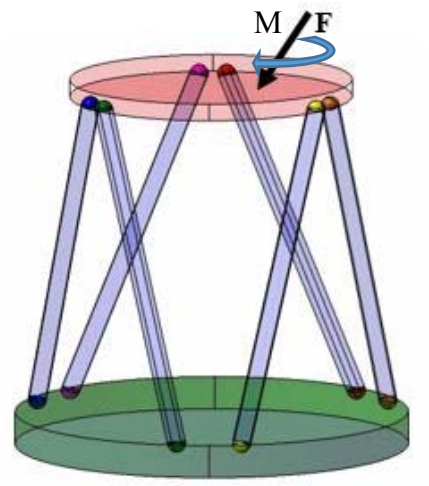

Figure: 4.2 CATIA Model of PI H-840

4.1 Data Input

During the analysis, the platform is considered not to be at its natural configuration. Initial length of each leg is given in table 4-2. Initial configuration of the platform in terms of YPR [1] is given in table 4-3. The orientation can be entered through spreadsheet. Other specifications are given in data sheet of PI H-840 drawing attached in Appendix A and also shown in table 4-1. These specifications are extracted from the drawing attached in Appendix. The material properties of Stewart platform and the machining forces acting on platform are also entered using spreadsheet. There could be any number of forces acting on platform but in specific case three simultaneous machining forces are being considered, shown in table 4-4 along with point of action of forces.

Arrangement angle of the legs at lower and upper plates, which is placement angle of legs at corresponding plate, could also be varied and is introduced in spreadsheet. To make a truss structure for stability of system, axis at base plate is taken at 0°, however, axis for platform are initially rotated at angle of 60° and for symmetry of system each leg at base is placed at angle of 10° and 6° at platform.

Table: 4-2 Initial leg lengths of Hexapod

Leg Length	Value (m)	Leg Length	Value (m)
l_1	0.315	l_4	0.310
l_2	0.311	l_5	0.293
l_3	0.320	l_6	0.284

[1] YRP: Yaw (α) Roll (β) Pitch (γ)

Table: 4-3 Initial Orientation of Platform

Axix	Angle (°)
X	7
Y	6
Z	5

Table: 4-4 Machining Forces and their positions

Force (N)	Force Position (mm)
{-15, -35, -65}	{0, 0, 283.35}
{-80, -65, -90}	{80, 80, 283.35}
{-45, -65, -95}	{-80, -80, 283.35}

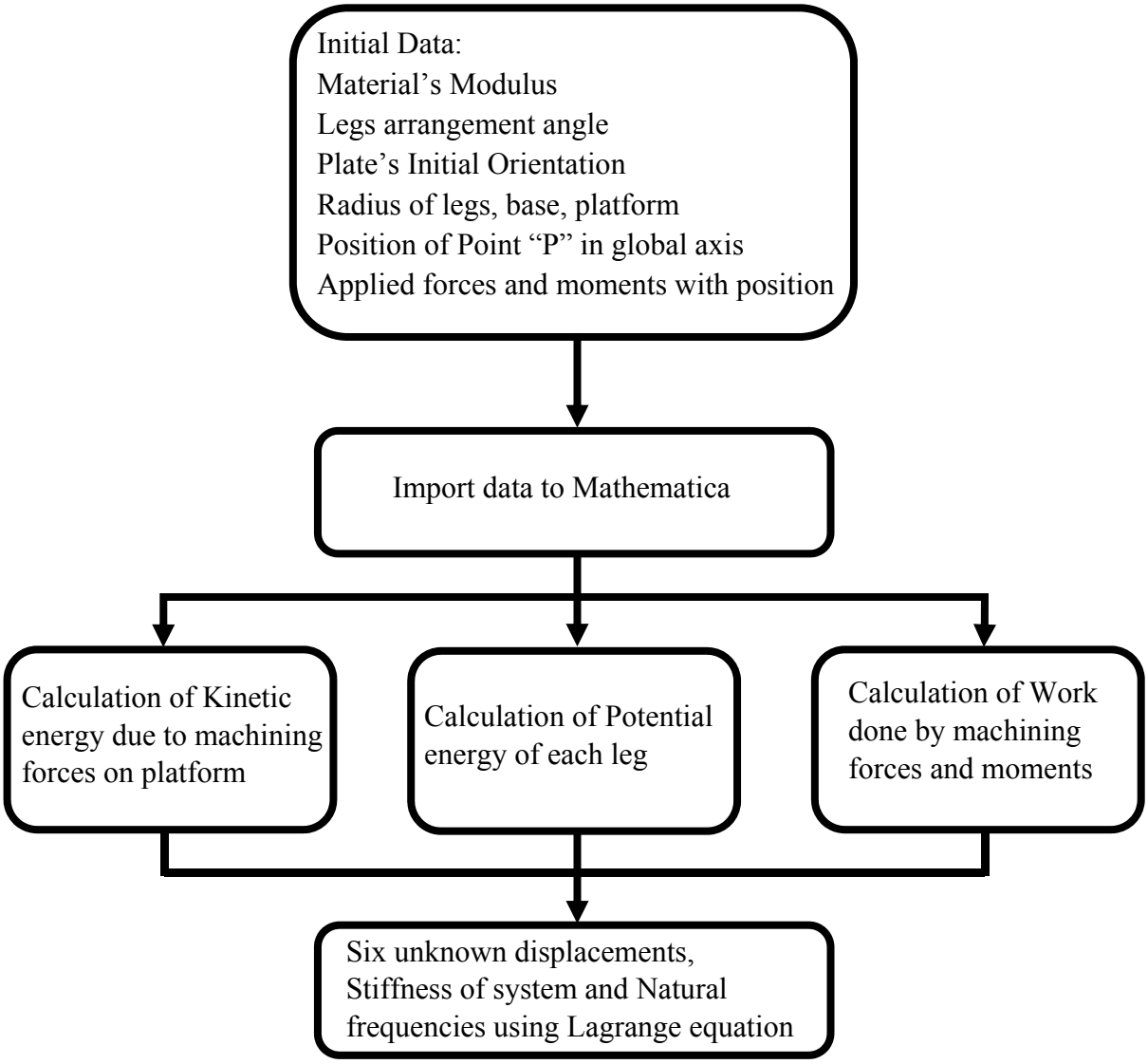

Figure: 4.3 Flow chart of proposed Mathematical Model

4.2 Working of Proposed Algorithm in Mathematica:

Main steps of proposed mathematical model are shown in figure 4-3. Each step is further explained in detail as follows:

4.2.1 Exporting Files:

Depending upon the input data i.e. number of forces and legs etc., the algorithm exports the required spreadsheet ".dat" files to enter the magnitude of forces being applied on platform, their point of action, moment (if any) being applied by the forces, the material properties including radius of leg, the arrangement angles of legs on the base and the platform, Initial orientation of platform (if any) and the imaginary point "P" that could be anywhere on the platform with reference to which all forces and positions of legs are defined, in the present case "P" is assumed to be the centre of gravity of the platform. These files are later imported by algorithm, so without entering the proper inputs the algorithm will not run any further.

4.2.2 Algorithm Calculation Flow:

In this section, the working of each step, given in figure 4-3, will be explained in detail.

4.2.2.1 Displacement Matrix:

The calculations start with calculation of RYP rotation matrix in which three rotations β, γ, and α are assumed along x, y and z axis. Multiplication of these rotations gives complete rotation matrix, further by assuming small angle assumption RYP is reduced to matrix shown in Eq. (3.10) and also shown below:

$$\begin{bmatrix} 1 & -\Delta\alpha & \Delta\gamma & \Delta X_P \\ \Delta\alpha & 1 & -\Delta\beta & \Delta Y_P \\ -\Delta\gamma & \Delta\beta & 1 & \Delta Z_P \\ 0 & 0 & 0 & 1 \end{bmatrix}$$

The simplified rotation matrix is used in all future calculations, like for calculation of displacement matrix which is obtained by subtraction of rotation matrix of point "P" from the simplified rotation matrix. As mentioned earlier the Point "P" is centre of gravity of platform so its rotation matrix is simply an identity matrix, the displacement matrix is shown in matrix of equation. 3.11 and also given below:

$$\begin{bmatrix} 0 & -\Delta\alpha & \Delta\gamma & \Delta X_P \\ \Delta\alpha & 0 & -\Delta\beta & \Delta Y_P \\ -\Delta\gamma & \Delta\beta & 0 & \Delta Z_P \\ 0 & 0 & 0 & 1 \end{bmatrix}$$

4.2.2.2 *Leg's coordinates and its length:*

To calculate the length of leg its coordinates at the platform and the base are required, which can be calculated using equation 3.2 and equation 3.3, which are also given below.

$$Lower\ coordinates\ = \begin{pmatrix} Radius\ of\ lower\ *\ cos\ \theta \\ Radius\ of\ lower\ *\ sin\ \theta \\ 0 \end{pmatrix}$$

$$Upper\ coordinates\ = \begin{pmatrix} \text{Radius of upper}\ *\ \cos\theta \\ \text{Radius of upper}\ *\ \sin\theta \\ \text{Z zxis of "P"} \end{pmatrix}$$

Now, that we have two coordinates of each leg, the calculated points can be used for calculation of length of leg using distance formula using equation 3.6, which is given as

$$Leg\ length = \sqrt{(x_1 - x_2)^2 + (y_1 - y_2)^2 + (z_1 - z_2)^2}$$

This length of leg plays an important role in upcoming calculations for evaluation of stiffness matrix of legs and its potential energy.

4.2.2.3 *Initial Orientation of Platform:*

The values of orientation of platform are imported from spreadsheet exported earlier, a rotation matrix again by using YRP rotation is constructed, this time it uses the values specified for orientation of platform. To add initial orientation of platform this constructed rotation matrix is multiplied with upper coordinates of legs calculated in equation 3.5 and also shown below. This multiplication with rotation matrix will increase or decrease the length of legs which will induce rotation in the platform. It should be noted that this rotation has no effect on the point "P" as point "P" is the reference point of this rotation.

$$Final\ Upper\ coordinates = \left(\begin{bmatrix} 1 & -\Delta\alpha & \Delta\gamma \\ \Delta\alpha & 1 & -\Delta\beta \\ -\Delta\gamma & \Delta\beta & 1 \end{bmatrix} . \begin{bmatrix} R_P\ *\ Cos\ \theta \\ R_P\ *\ Sin\ \theta \\ 0 \end{bmatrix} \right) + \begin{bmatrix} 0 \\ 0 \\ Z\ axis\ of\ "P" \end{bmatrix}$$

4.2.2.4 *Potential Energy of Leg:*

Potential energy of each leg is calculated using equation 3.7, area of each leg is same and is calculated using the radius from spreadsheet. For calculation of potential energy, we need the length of each leg, the length is used for calculation of unit vector using the length position vector and its magnitude, components of calculated unit vector are used in construction of stiffness matrix of each leg that is being treated as 3D truss. The stiffness matrices will be used for calculation of potential energy of each leg which is summed to get global PE of the hexapod. The overall PE will be used for calculation of stiffness matrix of system by derivation of potential energy w.r.t linear and angular velocities using equation 3.22a.

4.2.2.5 Kinetic Energy:

Although this is a static system so kinetic energy is zero because of absence of velocity of platform but the small amount of kinetic energy can be there due to applied machining forces on the platform with mass and inertia. The KE can be calculated using equation 3.18. Overall kinetic energy of platform includes linear and angular kinetic energies due to mass and inertia, respectively. This total kinetic energy will be used later for calculation of mass matrix of system by derivation of total kinetic energy w.r.t linear and angular velocities using equation 3.22b.

4.2.2.6 Work Calculation:

The imported force positons are taken with reference to point "P". This is done by calculating position vector of the force position with reference to point "P". To get the displaced force positions on the platform equation 3.20 is used, the force positions are multiplied with displacement matrix obtained in equation 3.11. Now, the linear work done is obtained by the scalar product of force vector and the calculated displacement matrix. To calculate overall linear work all linear works are added. The angular work is due to moment (if any) applied by the tool on the platform, the angular work is scalar product of moment vector with the angles β, γ, and α of platform. Total work done is summation of linear and angular works.

4.2.2.7 Lagrange and its solution:

The Lagrange equation requires the kinetic energy, potential energy and work done as inputs, but while solution of Lagrange for displacements of platform kinetic energy is "0". So the Lagrange equation will be simplified. By putting values in Lagrange, we get six equations with six unknowns, statically determinate problem. The solution will give six unknown variables that will be displacement of point "P" of platform.

$$\frac{\partial}{\partial t}\left(\frac{\partial(KE-PE)}{\partial \dot{q}_i}\right)-\frac{\partial(KE-PE)}{\partial q_i}-\frac{\partial W}{\partial q_i}=0$$

Displacements of any point in platform can be calculated using homogenous transformation matrix when its variables are replaced with displacements of point "P", the HTM is then multiplied with coordinates of that particular point of interest.

4.2.2.8 Natural frequencies:

Natural frequencies are calculated using mass matrix calculated in equation. 3.22b. Solution of equation. 3.22a gives the natural frequencies of platform. As it is a 6 DOF problem, six Natural frequencies will be calculated.

$|[M]^{-1}[K] - \omega^2[I]| = 0$

The Eigen values and Eigen vectors are calculated using the Eigenvalues and Eigenvectors command in Mathematica. The natural frequencies are obtained by taking square root of calculated Eigen values of system and the vector corresponding to each Eigen value gives the mode shape at that frequency.

4.3 Finite Element Analysis in CATIA:

The model with same dimension as that of provided by manufacturer of H-840 is modelled in CATIA for its FE analysis. Dimensions of the system are given in table 4-1, drawing provide by PI is attached in Appendix ("H-840 6-Axis Hexapod" 2016). Material of system is Aluminium few amendments are made in the material properties of different parts for better comparison between both the analysis in Mathematica and CATIA. Three parts of system are explained below.

4.3.1 Platform:

This is upper moveable plate with six spherical seats for fitting of legs, radius of each seat is 10mm. Each slot is coloured differently so that each leg is placed at its own side of global axis. Boolean command in CATIA is used for slots placement. The platform is 15mm thick. Material properties for this part is unchanged, default material properties provided by CATIA are used. The platform is shown in figure 4-4

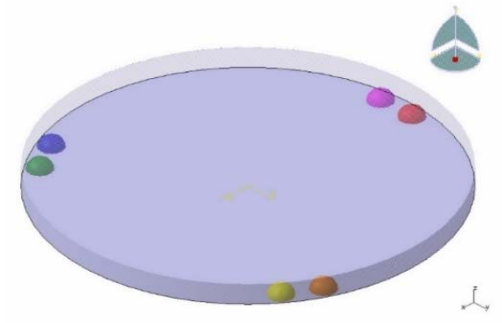

Figure: 4.4 Platform in CATIA

4.3.2 Base plate:

Like platform the base also have six slots for leg's sitting along with six different colours for each leg. The material properties for the base will not affect the analysis so these properties are also kept unchanged. The thickness of base is 29mm. Base is shown in figure 4-5

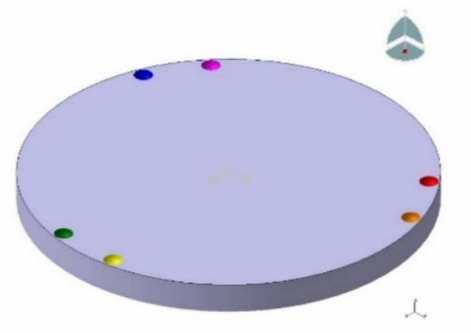

Figure: 4.5 Base plate in CATIA

4.3.3 Legs:

The only elastic bodied in analysis are legs. The length of leg changes with change in orientation of platform. For different configurations, the leg length changes each time and the values are taken from Mathematica calculations. To make legs massless, properties of material are modified in CATIA by changing density of Aluminium. Each leg is coloured differently according to its position in global axis, otherwise there are high chances of mistake which cause error in orientation of platform. Leg is shown in figure 4-6

Figure: 4.6 Leg in CATIA

4.3.4 Assembly:

All parts are designed separately in CATIA part design and assembled in assembly design. During the assembly, all legs are placed in proper pace in global axis and contact constraint is applied between each slot place at the platform and the base to upper and lower ends of legs, respectively. This contact constraint forms surface contact between legs and both the plates, as the result, plates have three angular degrees of freedom. Other three degrees of freedom can be provided manually by changing the length of legs, in real system prismatic joints with actuators are used for this purpose. 24 coloured squares show in figure 4-7 are surface contacts between plates and legs.

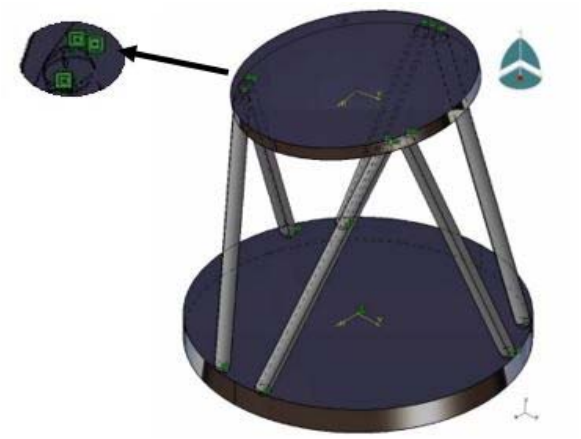

Figure: 4.7 Assembly of Stewart platform in CATIA

4.3.5 Analysis:

Analysis is performed in Generative Structural Analysis of CATIA, case for this analysis is Static Analysis. During the analysis, base plate is fixed for all kind of motions i.e. base has zero DOF. Both the base and the platform are made rigid from all side using "Rigid Virtual Part". The "User Defined Restrain" is used for complete rigid body motion of plates. "Rigid Connection Properties" are used for defining rigid connections between both the plates and all the legs.

Local points are imposed on platform to apply point loads and to obtain displacements of different points on the platform. As the platform is rigid so it is coarsely meshed with linear type elements, mesh size for base and platform is 16mm. Legs on the other hand are has 2mm mesh size with parabolic elements type. Applied machining forces are given in Table 3-3. This completes the requirements to run static analysis. The Stewart Platform ready for analysis is shown in figure 4-8.

4.3.6 Results for Displacements

The analysis is run to compute displacements of platform. First of all, the product is meshed according to size provided in last step, meshing time depends on the size of part and the number of elements. The meshed system is shown in figure 4-9. It can be observed that both platforms are coarsely meshed while legs are finer.

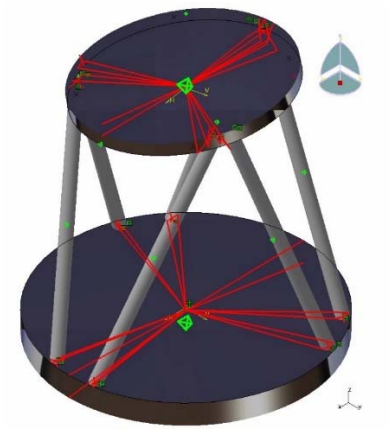

Figure: 4.8 Ready to run Analysis

Figure: 4.9 Meshed Stewart Platform

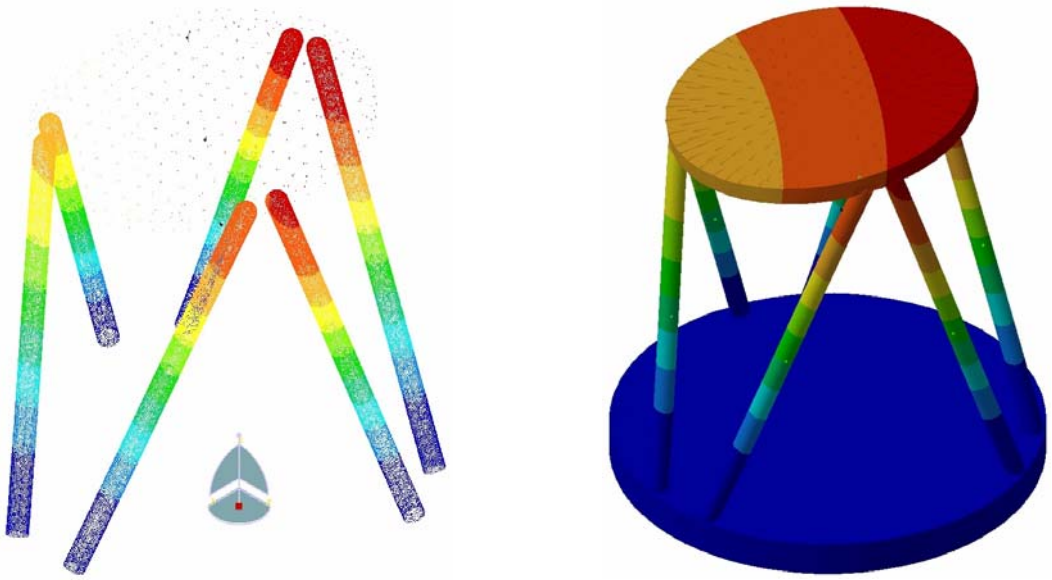

(a) Displacement (vector) Displacement (magnitude)

Figure: 4.10 Displacement Results of Analysis

For solution computation different available method can be selected, however, for this case auto solution method is used. Depending on the size of elements the solution time varies. The

translational displacement result for present case is shown in figure 4-10. Displacements obtained from Mathematica and CATIA for few selected point is given in table 4-5. The error magnitude column shows the percentage of magnitude of both displacement results obtained from FEA and analytical approach.

Table: 4-5 Displacement Results Comparison

Point (mm)	Displacements using Proposed method			Displacements using Simulation			Error's magnitude
	ΔX (μm)	ΔY (μm)	ΔZ (μm)	ΔX (μrad)	ΔY (μrad)	ΔZ (μrad)	
{0, 0, 283.35}	-6.441	-8.561	−1.098	-6.406	-8.328	-1.068	1.937%
{80, 80, 283.35}	-7.572	-7.430	-1.078	-7.697	-7.290	-1.212	-0.068%
{-80, 80, 283.35}	-7.572	-9.692	-1.457	-7.481	-9.550	-1.355	-1.441%
{-80, -80, 283.35}	-5.310	-9.692	-1. 118	-5.105	-9.412	-0.918	-2.836%
{80, -80, 283.35}	-5.310	-7.430	-7.387	-5.311	-7.09	-7.676	0.208%

4.3.7 3D Stiffness Matrix:

Final stiffness matrix is calculated using equation 3.22b, the calculated stiffness matrix is shown in equation 4.1.

$$\begin{bmatrix} 20.673 & 1.373 & -0.174 & -0.203 & 0.0557 & 0.313 \\ & 18.760 & 0.059 & -0.209 & -0.452 & 0.213 \\ & & 238.157 & -0.381 & -0.322 & 0.655 \\ & Symm. & & 1.597 & 0.033 & 0.025 \\ & & & & 1.570 & -0.033 \\ & & & & & 0.518 \end{bmatrix} x\ 10^6\ N/m \qquad (4.1)$$

4.4 Frequency Analysis in CATIA

For frequency analysis we need to select Frequency Analysis in "Generative Structural Analysis" rest of all steps are same as that of for static analysis. Before analysis the number of required mode shapes are changed to six. Six shapes of H-840 at first six natural frequencies are shown in figure 4-11, corresponding six Eigen vectors corresponding to the particular shapes are shown in equation 4.2. For better comparison of Eigen vectors and mode shapes Stewart platform is kept at its neutral configuration. Natural frequencies from Mathematica and CATIA are shown in table 4-6.

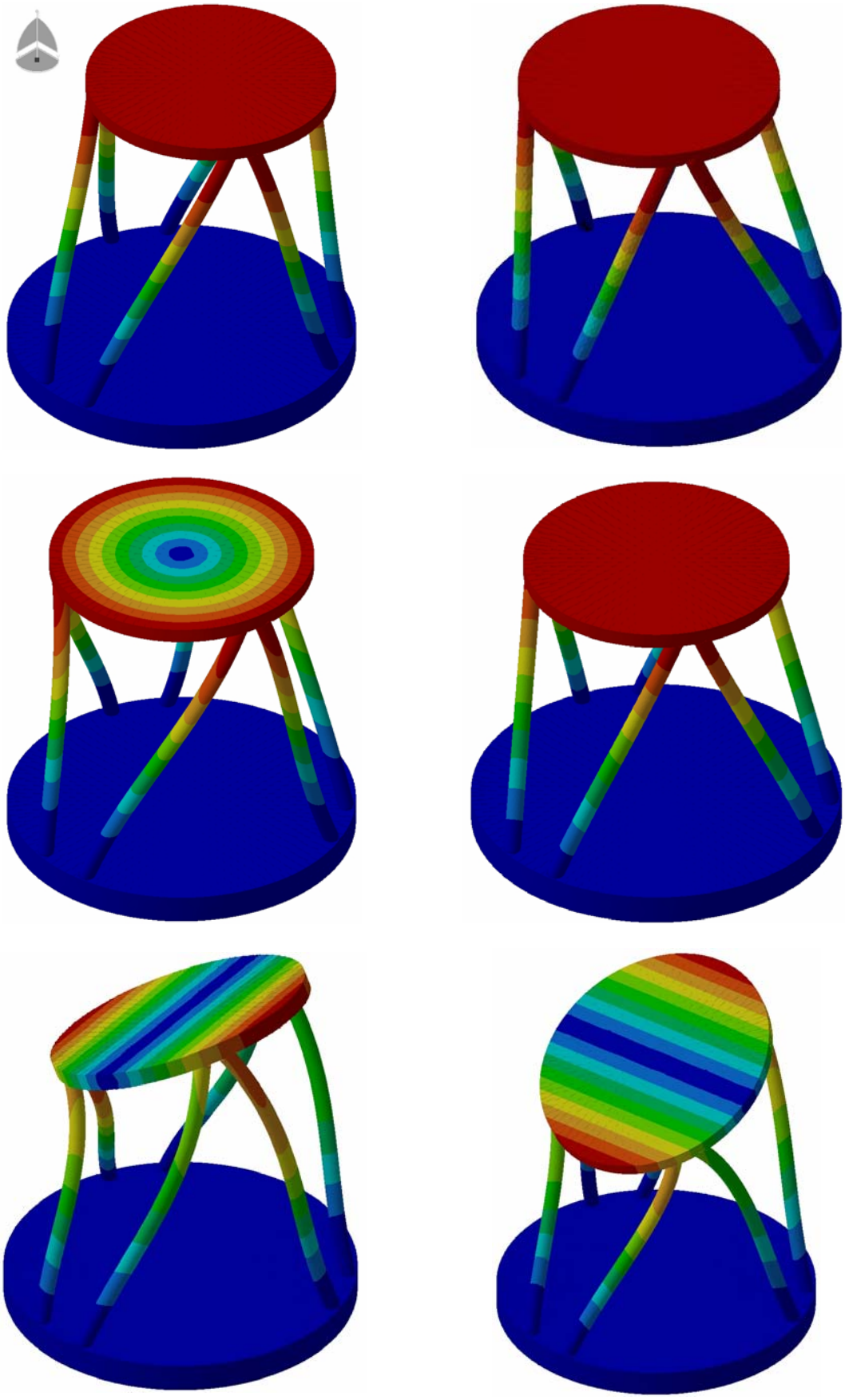

Figure: 4.11 Mode Shapes from CATIA

$$\begin{bmatrix} 0 & -996.313 & 0 & -85.791 & 0 & 0 \\ -996.313 & 0 & 0 & 0 & 85.790 & 0 \\ 0 & 0 & 0 & 0 & 0 & 1000 \\ 0 & 0 & 1000 & 0 & 0 & 0 \\ 0 & -0.348 & 0 & 1000 & 0 & 0 \\ -0.348 & 0 & 0 & 0 & -1000 & 0 \end{bmatrix} \tag{4.2}$$

Table: 4-6 Comparison of Natural Frequencies

Frequency (Hz)	Analytical	Simulation	% Error
ω_1	478.939	499.74	4.1
ω_2	517.687	499.742	3.5
ω_3	934.764	928.702	0.653
ω_4	1746.2	1726.52	1.14
ω_5	2214.83	2277.21	2.7
ω_6	2265.84	2278.37	0.558

4.5 Validation form Literature

Besides the validation of the proposed technique in the last section from Finite Element Analysis the work is validated by solving an example from Afzali – Far *et al.* (2014).

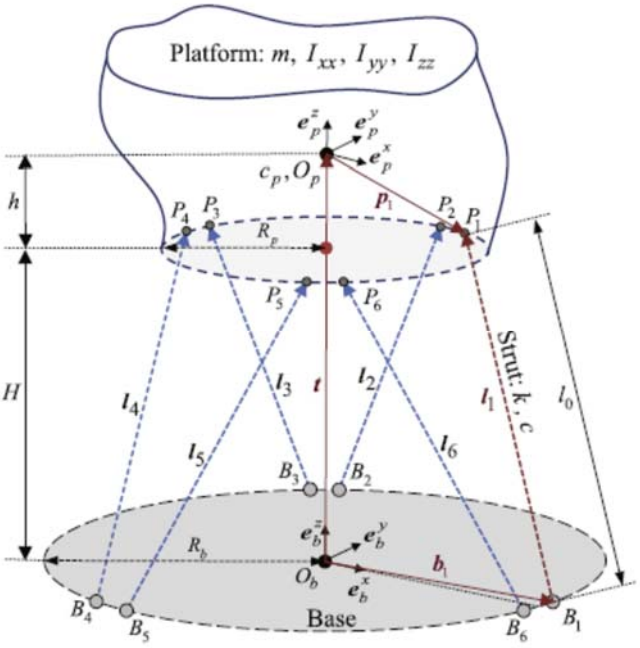

Figure: 4.12 Afzali - Far et al.'s GSP

Main aim of proposed analytical model in their work is to study the Inertia, damping and stiffness of the system that is useful in design and optimization of parallel manipulators especially hexapods like; Stewart Platform at its neutral configuration.

Afzali – Far *et al.* (2014) also applied Lagrangian formulation in his work to calculate the equation of motion of the system. Each leg is modelled as a linear spring with damper and results are calculated for both the damped and undamped system. The potential energy of each is calculated, the Kinetic energy of system is also calculated to calculate the Eigen values, Eigen vectors and Natural frequencies of system. The methodology is validated with FEA simulation in Ansys. In the end, the proposed methodology is applied to calculate the Stiffness matrix and Natural Frequencies of the Gough Stewart platform for collimation system of large optical telescope.

In this section, the mechanical model proposed in this thesis will be used to solve the same collimation system Gough Stewart Platform for Stiffness matrix and Natural frequencies and result from both the techniques will be compared to testify the mechanical model proposed in this thesis.

The inputs for benchmark work Afzali – Far *et al.* (2014) are extracted and converted into from more familiar with inputs introduced for mechanical model proposed in this thesis. The inputs are given in table 4-7.

Table: 4-7 Afzali - Far's Inputs

Symbol	Value	Symbol	Value
R_B	0.5m	H	0.9m
R_P	0.4m	θ_P	10˚
AE/L	10^6 N/m	θ_B	15˚

Using the inputs in table 4-7 and his proposed methodology Afzali – Far *et al.* calculated the stiffness matrix of system, shown in equation 4.3

$$[K]=\begin{bmatrix} 276820.2 & 0 & 0 & 0 & -16092.1 & 0 \\ 0 & 276820.2 & 0 & 16092.1 & 0 & 0 \\ 0 & 0 & 5446359.5 & 0 & 0 & 0 \\ 0 & 16.92.1 & 0 & 436158.9 & 0 & 0 \\ -16092.1 & 0 & 0 & 0 & 136158.9 & 0 \\ 0 & 0 & 0 & 0 & 0 & 88483.8 \end{bmatrix} N/m \quad (4.3)$$

Using same inputs in the algorithm proposed in this work and formulated in Mathematica the stiffness matrix is obtained which is shown in equation 4.4.

$$[K] = \begin{bmatrix} 279558 & 0 & 0 & 0 & -11704.5 & 0 \\ 0 & 279558 & 0 & 11704.5 & 0 & 0 \\ 0 & 0 & 5500230 & 0 & 0 & 0 \\ 0 & 11704.5 & 0 & 440018 & 0 & 0 \\ -11704.5 & 0 & 0 & 0 & 440018 & 0 \\ 0 & 0 & 0 & 0 & 0 & 89359 \end{bmatrix} N/m \quad (4.4)$$

Equation 4.5 gives the percentage error of both results

$$\begin{bmatrix} 0.98 & 0 & 0 & 0 & 27.26 & 0 \\ 0 & 0.98 & 0 & 27.26 & 0 & 0 \\ 0 & 0 & 0.98 & 0 & 0 & 0 \\ 0 & 27.26 & 0 & 0.88 & 0 & 0 \\ 27.26 & 0 & 0 & 0 & 0.88 & 0 \\ 0 & 0 & 0 & 0 & 0 & 0.98 \end{bmatrix} \quad (4.5)$$

By observing the equation 4.5, we can say that stiffness matrices obtained from both the techniques are very close, the diagonal terms are almost same with maximum percentage error just 0.98%, however, non-diagonal terms deviate from each other by 27.26%. As the analytical model of Afzali – Far *et al.* (2014) considers each leg to be a linear spring, a perpendicular force (or force other than axial axis) is applied at the ends of spring it causes bending in the spring. However, there is no bending error in the methodology proposed in this work because each leg is assumed to be a truss which does not bend under force. It should be noted that non diagonal terms are of less importance than that of diagonal terms, this statement will be proven by comparing the results of natural frequencies obtained by both the methods. Table 4-8 shows the Natural frequencies from Afzali's work and from model proposed in this work. Percentage error of Natural frequencies is shown in table 4-8.

Table: 4-8 Comparison of Natural Frequencies

Frequency (rad/s)	**Afzali -Far *et al.'s***	**Proposed Methodology**	**% Error**
ω_1	52.555	52.8428	0.54
ω_2	52.555	52.8428	0.54
ω_3	94.066	94.5299	0.49
ω_4	233.374	234.526	0.49
ω_5	295.361	296.659	0.43
ω_6	295.361	296.659	0.43

The maximum percentage error is just 0.54%, it should be noted that the stiffness matrix in equation 4.4 is used for calculation of Natural Frequencies in table 4-8. The repetitions of first

two and last two Natural Frequencies is due to neutral configuration of platform at which there is symmetry at x and y axis of platform.

So, we can conclude that the proposed methodology is valid for existing literature, it is worth mentioning that the methodology proposed in this work is more flexible than that of Afzali's because we can introduce separate value of radius of leg, material modulus of elasticity and different length of each leg of manipulator (calculated automatically form coordinates of point "P"), but Afzali *et al.* (2014) used direct value from axial loading of leg "AE/L = 10^6N/m".

4.6 Conclusion

In this chapter, the proposed methodology is applied on Stewart Platform that is commercially being fabricated. The specifications are taken from the manufacturer's online resources available for research purposes. Each step of the algorithm programmed in Mathematica, is explained form exporting of spreadsheet to final displacement and Natural frequencies calculations.

In the remaining sections, the parts' designing, their assembly, meshing and analysis are described for CATIA environment. All the necessary changes required to replicate the mathematical model in CATIA are described. The results from the proposed technique are compared with the simulation results. The proposed technique is also validated form recent literature. A numerical study is chosen from Afzali – Far *et al.*'s work, using their inputs and our methodology, we reproduce his results with minimum error.

CHAPTER 5: RESULTS AND DISCUSSIONS

In this chapter, graphical conclusion based on the results derived in last chapters will be deduced. The graphs are plotted by varying one design variable and keeping rests unaltered. This conclusion allows to predict the effect of single design variables (like; leg radius, legs placement angle and Modulus of Elasticity of material) on the positioning error of platform. It is worth mentioning, the platform is kept at neutral configuration during these plot.

5.1 Leg Angle vs Displacement

For this plot the leg's arrangement angle at the platform is varied keeping other design parameter constant. The leg's arrangement angle is varied from 2˚ to 10˚, other inputs are same as shown in Table 3-2. The force vector is {-500, -500, -500} at point "P" on the platform. The graph plotted for Leg angle vs the normalized value of six Displacements is shown in figure 5-1.

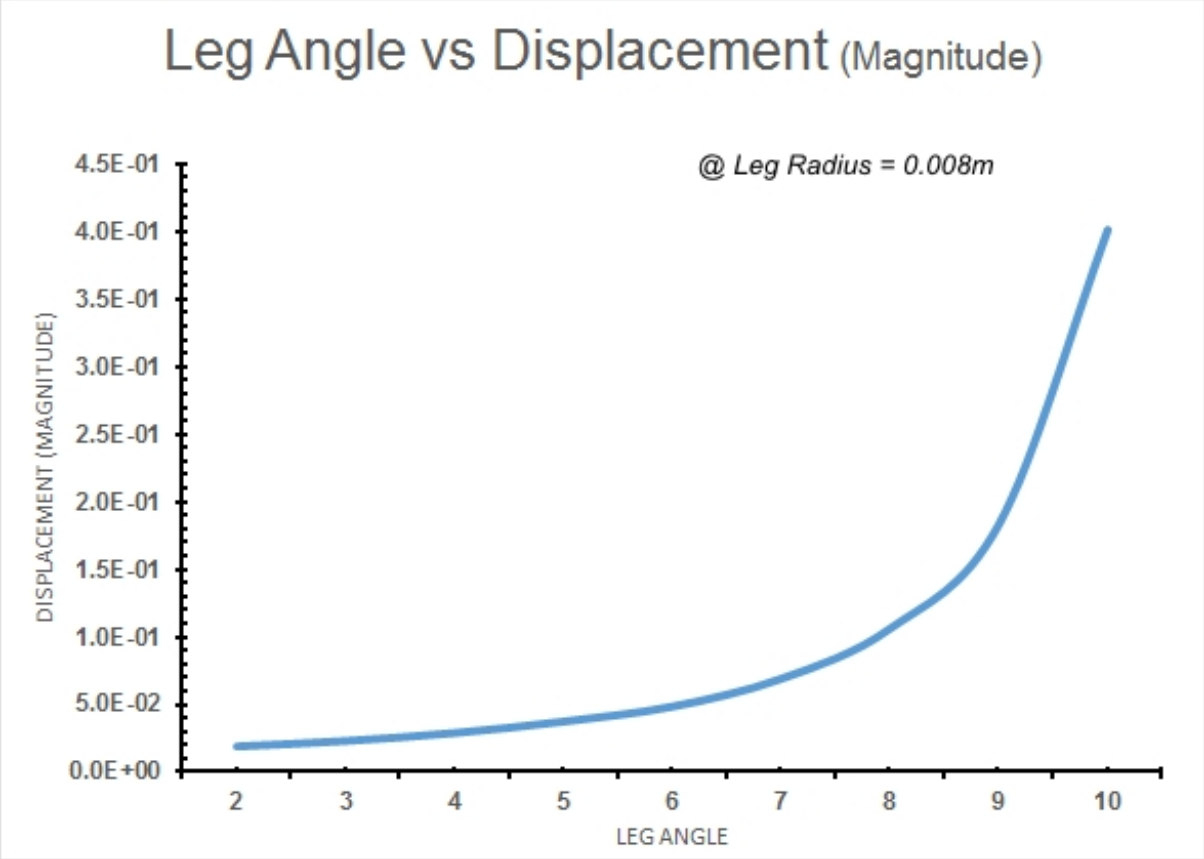

Figure: 5.1 Leg's Arrangement Angles vs Displacements

From figure 5-1 it can be observed that with decrease in leg angle there is decrease in displacement error of leg. Percentage decrease in positioning error with leg's arrangement angle from 10˚ to 9˚ is about 54%. The error will keep in decreasing with decrease in leg angle,

but the error trend becomes less steep after 6˚ leg arrangement angle. It is also important to note that the leg angle and leg radius (next plot) are interdependent of each other.

5.2 Leg Radius vs Displacements

For this plot the leg radius is varied keeping other design parameter constant. The leg radius is varied from 5mm to 12mm, other inputs are same as that of for the previous plot. The graph plotted for Leg radius vs Displacements is shown in figure 5-2.

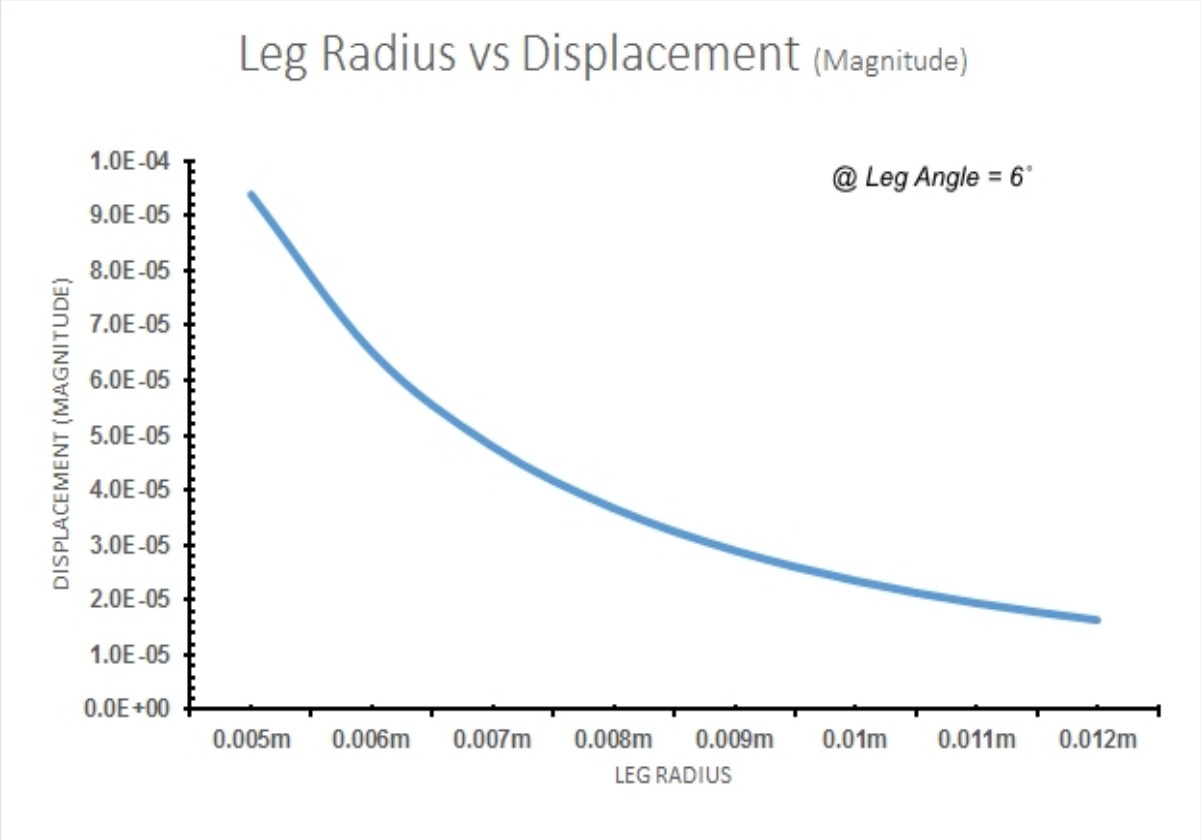

Figure: 5.2 Leg's Radius vs Displacements

From figure 5-2, it can be observed that as the leg radius is increased there is decrease in normalized displacement error of platform under force, in the beginning there is more rapid decrease in displacement error per mm increase in radius of leg, which later becomes less steep per mm increase in leg radius like; for increase in leg radius from 5mm to 6mm there is 30% decrease in normalized displacement error of platform while the percentage error decrease with radius increase from 11mm to 12mm is just 16%. Another important conclusion that can be deduced from figure 5-1 and figure 5-2 is that leg radius cannot be increase beyond certain limit because with increase in leg radius there will be increase in leg angle which will again increase the displacement error. So an optimization according to requirements is needed. Another thing that can be done is using the "Modified Stewart Platform" in which leg at upper

platform are connected in two circles instead of one, but this design of Stewart platform has lower working envelop and torque carrying capability than that of original design (Stoughton and Arai 1993).

5.3 Modulus of Elasticity vs Displacement

During this plot, the modulus of elasticity of material is varied from 10GPa to 400GPa. Plot of normalized value of displacement and modulus of material is shown in figure 5-3.

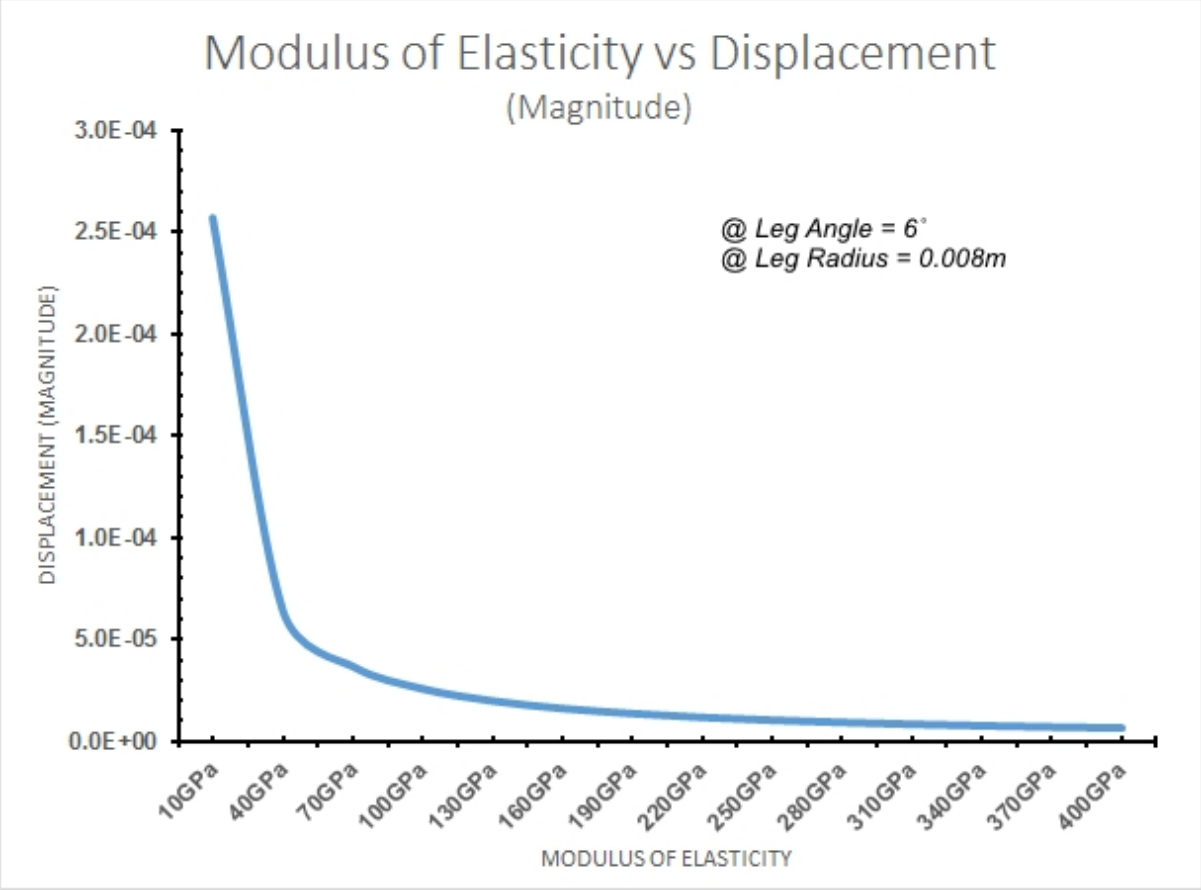

Figure: 5.3 Modulus of Elasticity of Material vs Normalized Displacements

From the plot it can be observed that at modulus of value 70GPa displacement curve becomes smooth. So Aluminium can be selected as design material for hexapod with specification given in table 4-1. If steel is selected as material for the Hexapod (200GPa) the displacement error will be almost 28% less than that of the system designed with Aluminium as material.

5.4 Conclusion

From the graphical results, it can be concluded that different variables depend on each other. In figure 5-1, the arrangement angle of leg at the platform is directly proportional to the magnitude of displacement of the platform, but the arrangement angle cannot be

decreased beyond certain limits due to its dependency on the legs radius. The displacement is inversely proportional to the leg radius, which cannot be increased above certain level because greater the radius of leg greater will be the placement angle between two legs at the platform. Form figure 5-3, the importance of modulus of elasticity of material can be observed, so atleast Aluminium or harder metal should be used form fabrication of Hexapod with specification given in table 4-1.

CHAPTER 6: CONCLUSION AND FUTURE WORKS

This work is placed in the field of precision manufacturing. The thesis consists of formulating a mathematical model which allows the calculation of displacement error in position of platform of hexapod due to application of external machining forces and moments. The position of platform is taken with respect to an imaginary point "P" that is assumed to be the centre of gravity of platform. The point "P" is further taken in global coordinates. In the proposed mathematical model, each leg is assumed to be a 3D truss body attached to two point at upper platform and the base. The assumption of leg as truss is due to spherical joint between plates and legs.

During the calculations, only legs are elastic bodies everything else like platform, base and joints between legs and platform are absolute rigid bodies, so it is expected that due to applied machining forces, there will be some displacement error in position of platform due to elasticity of legs. This displacement error is calculated using Lagrange formulation. The equation requires potential energy, kinetic energy and work done all in terms of six unknown variables, as input and calculates the displacements of platform. During this thesis, it is assumed that hexapod is at static when machining forces are applied on it so the kinetic energy term will be zero because of no velocity. Later the kinetic energy term is included which is due to mass of the platform when machining forces are applied at it. The kinetic energy is then used to calculated the natural frequencies of hexapod. The proposed model is programmed in MATHEMATICA® and is totally generic for number of legs and forces applied on the platform.

This work is validated literature and working is explained and verified by finite element analysis designed and modelled in CATIA. Results from both techniques are very close. As compared to the FE analysis results produced using proposed technique are quick. Time taken by MATHEMATICA® to produce results in table 4-5 is just 1.234 seconds, while time used by CATIA® for same model is about 30 minutes on same system and this time for FE simulation will increase with increase in size of model while time will not be affected much in MATHEMATICA®.

The proposed future works for the current research includes:

(a) Joint's flexibility and clearance are also accountable for the positioning error in the platform of manipulator, so in future clearance and flexibility of the joints can be studied.

(b) The proposed algorithm is for static system which can be enhanced to dynamic system.
(c) Experimental validation of the proposed model is yet to be done.
(d) The work can be further improved by considering damping in the legs.

APPENDIX A

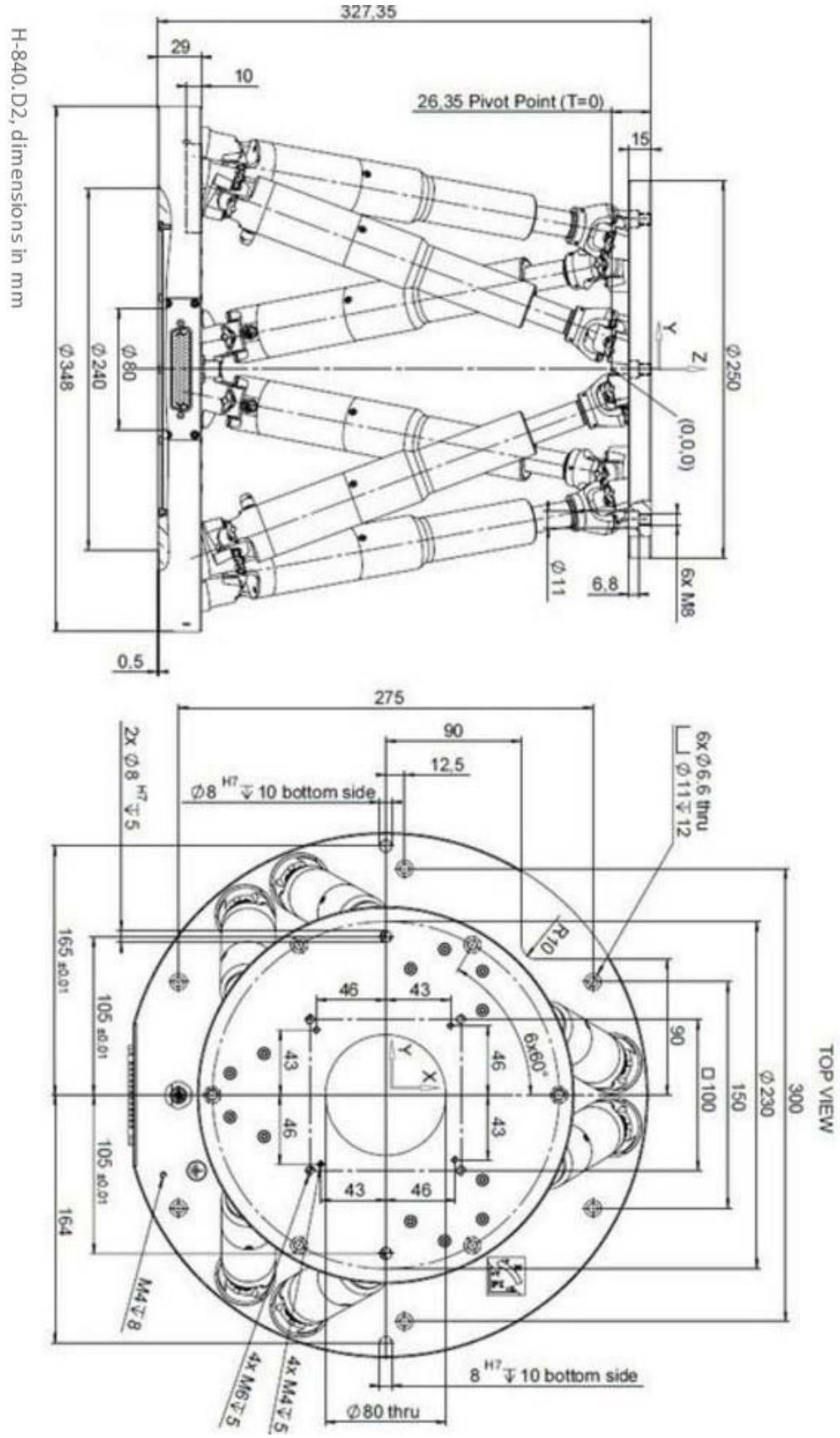
H-840.D2, dimensions in mm
327.35
29
10
26.35 Pivot Point (T=0)
15
Ø348
Ø240
Ø80
Ø250
(0,0,0)
Ø11
6.8
6x M8
0.5
275
90
12.5
2x Ø8 H7 ↧5
Ø8 H7 ↧10 bottom side
6xØ6.6 thru
Ø11↧12
R10
165 ±0.01
105 ±0.01
105 ±0.01
164
46
43
6x60°
90
□100
150
Ø230
300
TOP VIEW
M4↧8
4x M6↧5
4x M4↧5
8 H7 ↧10 bottom side
Ø80 thru

REFERENCES

Ahmad, Aftab, Kjell Andersson, Ulf Sellgren, and Suleman Khan. 2014. "A Stiffness Modeling Methodology for Simulation-Driven Design of Haptic Devices." *Engineering with Computers* 30 (1): 125–141.

Bennett, David J., Davi Geiger, and John M. Hollerbach. 1991. "Autonomous Robot Calibration for Hand-Eye Coordination." *The International Journal of Robotics Research* 10 (5): 550–559.

Bera, T. C., K. A. Desai, and P. V. M. Rao. 2011. "Error Compensation in Flexible End Milling of Tubular Geometries." *Journal of Materials Processing Technology* 211 (1): 24–34.

Bogdan, Ioana-Corina, and Gabriel Abba. 2009. "Identification of the Servomechanism Used for Micro-Displacement." http://sam.ensam.eu/handle/10985/8931.

Butt, Sajid Ullah, Jean-Francois Antoine, and Patrick Martin. 2013. "A Kinematic Approach for 6-DOF Part Positioning." In *Smart Product Engineering*, 147–157. Springer. http://link.springer.com/chapter/10.1007/978-3-642-30817-8_15.

Carbone, Giuseppe. 2011. "Stiffness Analysis and Experimental Validation of Robotic Systems." *Frontiers of Mechanical Engineering* 6 (2): 182–196.

Chablat, Damien, and Philippe Wenger. 2003. "Architecture Optimization of a 3-DOF Translational Parallel Mechanism for Machining Applications, the Orthoglide." *Robotics and Automation, IEEE Transactions on* 19 (3): 403–410.

Cheboxarov, V. V., V. F. Filaretov, and M. Vukobratović. 2000. "Raising the Stiffness of Manipulators with Lightweight Links." *Mechanism and Machine Theory* 35 (1): 1–13.

Chen, S., and I. Kao. 1999. "The Conservative Congruence Transformation of Stiffness Control in Robotic Grasping and Manipulation." In *Proceedings of the 9th International Symposium of Robotics Research*, 7–14.

Ciblak, Namik, and Harvey Lipkin. 1999. "Synthesis of Cartesian Stiffness for Robotic Applications." In *Robotics and Automation, 1999. Proceedings. 1999 IEEE International Conference on*, 3:2147–2152. IEEE. http://ieeexplore.ieee.org/xpls/abs_all.jsp?arnumber=770424.

Clinton, Charles M., Guangming Zhang, and Albert J. Wavering. 1997. "Stiffness Modeling of a Stewart Platform Based Milling Machine." http://drum.lib.umd.edu/handle/1903/5859.

Corradini, Charles, Jean-Christophe Fauroux, S. Krut, and others. 2003. "Evaluation of a 4-Degree of Freedom Parallel Manipulator Stiffness." In *Proceedings of the 11th World*

Congress in Mechanisms and Machine Science, Tianjin (China). http://www.lirmm.fr/krut/internal-pdf://2003_corradini_wcmms-4291545856/2003_corradini_wcmms.pdf.

Cui, Hongliang, and Zhenqi Zhu. 2006. *Error Modeling and Accuracy of Parallel Industrial Robots*. INTECH Open Access Publisher. http://cdn.intechopen.com/pdfs/382.pdf.

Daney, David, Nicolas Andreff, Gilles Chabert, and Yves Papegay. 2006. "Interval Method for Calibration of Parallel Robots: Vision-Based Experiments." *Mechanism and Machine Theory* 41 (8): 929–944.

Deblaise, Dominique, Xavier Hernot, and Patrick Maurine. 2006. "A Systematic Analytical Method for PKM Stiffness Matrix Calculation." In *Robotics and Automation, 2006. ICRA 2006. Proceedings 2006 IEEE International Conference on*, 4213–4219. IEEE. http://ieeexplore.ieee.org/xpls/abs_all.jsp?arnumber=1642350.

Dolinsky, Jens-Uwe, I. D. Jenkinson, and G. J. Colquhoun. 2007. "Application of Genetic Programming to the Calibration of Industrial Robots." *Computers in Industry* 58 (3): 255–264.

Dombiak, P., M. Shoham, and G. Grossman. 2000. "A Parallel Six Degrees-of-Freedom Inflatable Robot." In *ASME Mechanism and Robotics Conference Baltimore*.

Dow, Thomas A., Edward L. Miller, and Kenneth Garrard. 2004. "Tool Force and Deflection Compensation for Small Milling Tools." *Precision Engineering* 28 (1): 31–45.

Duffy, Joseph. 1996. *Robotics and Kinematics with Applications to Robotics*. Cambridge University Press, Cambridge.

DUKKIPATI, V. RAO, and J. Srinivas. 2012. *Textbook of Mechanical Vibrations*. PHI Learning Pvt. Ltd. https://books.google.com.pk/books?hl=en&lr=&id=JQkDEYvAGDAC&oi=fnd&pg=PR2&dq=textbook+of+mechanical+vibrations+rao+v+dukkipati+second+edition&ots=J38yUlICjm&sig=3p6ELpqeZx2qVIdM8KF2TPSgx08.

Elatta, A. Y., Li Pei Gen, Fan Liang Zhi, Yu Daoyuan, and Luo Fei. 2004. "An Overview of Robot Calibration." *Information Technology Journal* 3 (1): 74–78.

El-Khasawneh, Bashar S., and Placid M. Ferreira. 1999. "Computation of Stiffness and Stiffness Bounds for Parallel Link Manipulators." *International Journal of Machine Tools and Manufacture* 39 (2): 321–342.

Geldart, Martin, Phil Webb, Hans Larsson, M. Backstrom, Noel Gindy, and Kjell Rask. 2003. "A Direct Comparison of the Machining Performance of a Variax 5 Axis Parallel

Kinetic Machining Centre with Conventional 3 and 5 Axis Machine Tools." *International Journal of Machine Tools and Manufacture* 43 (11): 1107–1116.

Gong, Chunhe, Jingxia Yuan, and Jun Ni. 2000. "Nongeometric Error Identification and Compensation for Robotic System by Inverse Calibration." *International Journal of Machine Tools and Manufacture* 40 (14): 2119–2137.

Gosselin, C. M., and D. Zhang. 2002. "Stiffness Analysis of Parallel Mechanisms Using a Lumped Model." *International Journal of Robotics and Automation* 17 (1): 17–27.

Gosselin, Clement. 1990. "Stiffness Mapping for Parallel Manipulators." *Robotics and Automation, IEEE Transactions on* 6 (3): 377–382.

Gough, V. E., and S. G. Whitehall. 1962. "Universal Tyre Test Machine." In *Proc. FISITA 9th Int. Technical Congress*, 117–137. http://www.mecademic.com/references/Gough.pdf.

"H-840 6-Axis Hexapod." 2016. Accessed March 14. http://www.physikinstrumente.com/product-detail-page/h-840-700810.html.

Hernez, E., S.I. Valdez, and E. Sanchez. 2014. "On the Numerical Modelling and Error Compensation for General Gough-Stewart Platform." *International Journal of Advanced Robotic Systems* 11. doi:10.5772/58849.

Hollerbach, John, Wisama Khalil, and Maxime Gautier. 2008. "Model Identification." In *Springer Handbook of Robotics*, 321–344. Springer. http://link.springer.com/10.1007/978-3-540-30301-5_15.

Horin, Ben. n.d. "P., 1999,'Analysis and Synthesis of an Inflatable Parallel Robot.'" M. Sc. Thesis, Technion, Haifa.

Hu, Xiao, Rencheng Wang, Fangfang Wu, Dewen Jin, Xiaohong Jia, Jichuan Zhang, Fuwen Cai, and Shuangxi Zheng. 2007. "Finite Element Analysis of a Six-Component Force Sensor for the Trans-Femoral Prosthesis." In *Digital Human Modeling*, 633–639. Springer. http://link.springer.com/chapter/10.1007/978-3-540-73321-8_72.

Huang, Tian, Xingyu Zhao, and David J. Whitehouse. 2002. "Stiffness Estimation of a Tripod-Based Parallel Kinematic Machine." *Robotics and Automation, IEEE Transactions on* 18 (1): 50–58.

Kao, Inmin, and Chi Ngo. 1999. "Properties of the Grasp Stiffness Matrix and Conservative Control Strategies." *The International Journal of Robotics Research* 18 (2): 159–167.

Kevin, L., P. Conrad, and S. Shiakolas. 2000. "Robotic Calibration Issues: Accuracy, Repeatability and Calibration." In *Mediterranean Conference on Control & Automation, Greece*.

Khalil, Wisama, and Sébastien Besnard. 2002. “Geometric Calibration of Robots with Flexible Joints and Links.” *Journal of Intelligent and Robotic Systems* 34 (4): 357–379.

Kim, J., Changfaeom Park, Jongwon Kim, and F. C. Park. 1997. “Performance Analysis of Parallel Manipulator Architectures for CNC Machining Applications.” In *Proc. IMECE Symp. On Machine Tools, Dallas*.

Klimchik, Alexandr. 2011. “Enhanced Stiffness Modeling of Serial and Parallel Manipulators for Robotic-Based Processing of High Performance Materials.” Ecole Centrale de Nantes (ECN)(ECN)(ECN)(ECN); Ecole des Mines de Nantes. https://tel.archives-ouvertes.fr/tel-00711978/.

Kövecses, J., and J. Angeles. 2007. “The Stiffness Matrix in Elastically Articulated Rigid-Body Systems.” *Multibody System Dynamics* 18 (2): 169–184.

Lalanne, Michel, Patrick Berthier, and Johan Der Hagopian. 1986. *Mécanique Des Vibrations Linéaires (Avec Exercices Corrigés et Programmes de Calcul)*. Masson. http://infoscience.epfl.ch/record/60508.

Lebret, Guy, Kai Liu, and Frank L. Lewis. 1993. “Dynamic Analysis and Control of a Stewart Platform Manipulator.” *Journal of Robotic Systems* 10 (5): 629–655.

Li, Yu-Wen, Jin-Song Wang, and Li-Ping Wang. 2002. “Stiffness Analysis of a Stewart Platform-Based Parallel Kinematic Machine.” In *Robotics and Automation, 2002. Proceedings. ICRA’02. IEEE International Conference on*, 4:3672–3677. IEEE. http://ieeexplore.ieee.org/xpls/abs_all.jsp?arnumber=1014280.

Lin, Lin, Chao Yang, Jianfeng Lu, and Lexing Ying. 2011. “A Fast Parallel Algorithm for Selected Inversion of Structured Sparse Matrices with Application to 2d Electronic Structure Calculations.” *SIAM Journal on Scientific Computing* 33 (3): 1329–1351.

Long, Craig Stephen, J. A. Snyman, and A. A. Groenwold. 2003. “Optimal Structural Design of a Planar Parallel Platform for Machining.” *Applied Mathematical Modelling* 27 (8): 581–609.

Mahboubkhah, M., M. J. Nategh, and S. Esmaeilzadeh Khadem. 2009. “A Comprehensive Study on the Free Vibration of Machine Tools’ Hexapod Table.” *The International Journal of Advanced Manufacturing Technology* 40 (11–12): 1239–1251.

Majou, F. 2004. “Kinetostatic Analysis of Translational Parallel Kinematic Machines.” Ph. D. thesis, Universite Laval, Quebec, Canada and Ecole Centrale Nantes, France.

Majou, Félix, Clément Gosselin, Philippe Wenger, and Damien Chablat. 2007. “Parametric Stiffness Analysis of the Orthoglide.” *Mechanism and Machine Theory* 42 (3): 296–311.

Meggiolaro, Marco A., Steven Dubowsky, and Constantinos Mavroidis. 2005. “Geometric and Elastic Error Calibration of a High Accuracy Patient Positioning System.” *Mechanism and Machine Theory* 40 (4): 415–427.

Merlet, J. P. 2000. “Parallel RobotsKluwer Academic Publishers.” *Dordrecht, The Netherlands*.

Mirman, C. R., and K. C. Gupta. 1992. “Compensation of Robot Joint Variables Using Special Jacobian Matrices.” *Journal of Robotic Systems* 9 (1): 113–137.

Nagai, Kiyoshi, and Zhengyong Liu. 2007. “A Systematic Approach to Stiffness Analysis of Parallel Mechanisms and Its Comparison with FEM.” In *SICE, 2007 Annual Conference*, 1087–1094. IEEE. http://ieeexplore.ieee.org/xpls/abs_all.jsp?arnumber=4421146.

Pashkevich, Anatol, Damien Chablat, and Philippe Wenger. 2009. “Stiffness Analysis of Overconstrained Parallel Manipulators.” *Mechanism and Machine Theory* 44 (5): 966–82. doi:10.1016/j.mechmachtheory.2008.05.017.

Pashkevich, Anatol, Alexandr Klimchik, and Damien Chablat. 2011. “Enhanced Stiffness Modeling of Manipulators with Passive Joints.” *Mechanism and Machine Theory* 46 (5): 662–79. doi:10.1016/j.mechmachtheory.2010.12.008.

Paziani, Fabricio Tadeu, Benedito Di Giacomo, and Roberto Hideaki Tsunaki. 2009. “Robot Measuring Form Errors.” *Robotics and Computer-Integrated Manufacturing* 25 (1): 168–177.

Pierrot, F., P. Dauchez, and A. Fournier. 1991. “HEXA: A Fast Six-DOF Fully-Parallel Robot.” In *Advanced Robotics, 1991.’Robots in Unstructured Environments’, 91 ICAR., Fifth International Conference on*, 1158–1163. IEEE. http://ieeexplore.ieee.org/xpls/abs_all.jsp?arnumber=240399.

Pierrot, Francois, Vincent Nabat, Olivier Company, Sébastien Krut, and Philippe Poignet. 2009. “Optimal Design of a 4-Dof Parallel Manipulator: From Academia to Industry.” *Robotics, IEEE Transactions on* 25 (2): 213–224.

Pigoski, T., M. Griffis, and J. Duffy. 1998. “Stiffness Mappings Employing Different Frames of Reference.” *Mechanism and Machine Theory* 33 (6): 825–838.

Piras, Gabriel, W. L. Cleghorn, and J. K. Mills. 2005. “Dynamic Finite-Element Analysis of a Planar High-Speed, High-Precision Parallel Manipulator with Flexible Links.” *Mechanism and Machine Theory* 40 (7): 849–862.

Portman, Vladimir T. 2000. *Stiffness and Damping in Mechanical Design*. Elsevier.

Ramesh, R, M. A Mannan, and A. N Poo. 2000. “Error Compensation in Machine Tools — a Review: Part I: Geometric, Cutting-Force Induced and Fixture-Dependent Errors.” *International Journal of Machine Tools and Manufacture* 40 (9): 1235–56. doi:10.1016/S0890-6955(00)00009-2.

Rehsteiner, F., R. Neugebauer, S. Spiewak, and F. Wieland. 1999. “Putting Parallel Kinematics Machines (PKM) to Productive Work.” *CIRP Annals-Manufacturing Technology* 48 (1): 345–350.

Roth, ZVIS, B. Mooring, and Bahram Ravani. 1987. “An Overview of Robot Calibration.” *IEEE Journal on Robotics and Automation* 5 (3): 377–385.

Ruggiu, Maurizio. 2012. “On the Lagrangian and Cartesian Stiffness Matrices of Parallel Mechanisms with Elastic Joints.” *Advanced Robotics* 26 (1–2): 137–153.

Salisbury, J. Kenneth. 1980. “Active Stiffness Control of a Manipulator in Cartesian Coordinates.” In *Decision and Control Including the Symposium on Adaptive Processes, 1980 19th IEEE Conference on*, 95–100. IEEE. http://ieeexplore.ieee.org/xpls/abs_all.jsp?arnumber=4046624.

Shoval, Shraga, and Moshe Shoham. 2001. “Sensory Redundant Parallel Mobile Mechanism.” In *Robotics and Automation, 2001. Proceedings 2001 ICRA. IEEE International Conference on*, 3:2273–2278. IEEE. http://ieeexplore.ieee.org/xpls/abs_all.jsp?arnumber=932961.

Stewart, D. 1965. “A Platform with Six Degrees of Freedom.” *Proceedings of the Institution of Mechanical Engineers* 180 (1): 371–86. doi:10.1243/PIME_PROC_1965_180_029_02.

Stoughton, Robert S., and Tatsuo Arai. 1993. “A Modified Stewart Platform Manipulator with Improved Dexterity.” *Robotics and Automation, IEEE Transactions on* 9 (2): 166–173.

Tlusty, Jiri, John Ziegert, and Shannon Ridgeway. 1999. “Fundamental Comparison of the Use of Serial and Parallel Kinematics for Machines Tools.” *CIRP Annals-Manufacturing Technology* 48 (1): 351–356.

Toyama, Taizo, Yoichi Yamakawa, and Hiroyoshi Suzuki. 1998. *Machine Tool Having Parallel Structure*. Google Patents. https://www.google.com/patents/US5715729.

Tsai, Lung-Wen, and Sameer Joshi. 2000. “Kinematics and Optimization of a Spatial 3-UPU Parallel Manipulator.” *Journal of Mechanical Design* 122 (4): 439–446.

Veitschegger, William K., and Chi-Haur Wu. 1986. “Robot Accuracy Analysis Based on Kinematics.” *Robotics and Automation, IEEE Journal of* 2 (3): 171–179.

Watanabe, A., S. Sakakibara, K. Ban, M. Yamada, G. Shen, and T. Arai. 2006. “A Kinematic Calibration Method for Industrial Robots Using Autonomous Visual Measurement.” *CIRP Annals-Manufacturing Technology* 55 (1): 1–6.

Wenger, Ph, C. Gosselin, and B. Maille. 1999. “A Comparative Study of Serial and Parallel Mechanism Topologies for Machine Tools.” *Proceedings of PKM* 99: 23–32.

Wenger, Philippe, Clément Gosselin, and Damien Chablat. 2007. “A Comparative Study of Parallel Kinematic Architectures for Machining Applications.” *arXiv Preprint arXiv:0707.3665*. http://arxiv.org/abs/0707.3665.

Yi, Byung-Ju, and Robert A. Freeman. 1993. “Geometric Analysis of Antagonistic Stiffness in Redundantly Actuated Parallel Mechanisms.” *Journal of Robotic Systems* 10 (5): 581–603.

Zhang, Dan. 2001. *Kinetostatic Analysis and Optimization of Parallel and Hybrid Architectures for Machine Tools*.

Zhang, Dan, and Lihui Wang. 2005. “Conceptual Development of an Enhanced Tripod Mechanism for Machine Tool.” *Robotics and Computer-Integrated Manufacturing* 21 (4): 318–327.

CERTIFICATE OF COMPLETENESS

It is hereby certified that the dissertation submitted by NS Muhammad Sohail, Reg No. NUST201362430MCEME35113F, Titled: *Application of Lagrangian Formulation to Predict the Positioning Error of Parallel Manipulator Under External Loads* has been checked/reviewed and its contents are complete in all respects.

Supervisor's Name: Dr. Sajid Ullah Butt Signature: _____

Date: _____